G.E.C. Journal

VOL. XVII APRIL, 1950 No. 2

CONTENTS

PAGE

FRONTISPIECE—STRUCTURE TESTING AT THE R.A.E., FARNBOROUGH - - - 58

KOEPE WINDERS - - - - - - - - - - - - - 59
By A. B. Price

X-RAYS IN THE DEVELOPMENT OF INORGANIC PHOSPHORS - - - - 89
By H. P. Rooksby and A. H. McKeag

STRUCTURE TESTING EQUIPMENT AT THE ROYAL AIRCRAFT ESTABLISHMENT, FARNBOROUGH - - - - - - - - - - - - 96
By S. A. G. Emms

TECHNICAL LITERATURE - - - - - - - - - - - - 104

Published by

THE GENERAL ELECTRIC COMPANY LIMITED
Magnet House, Kingsway, London, England.

COPYRIGHT.

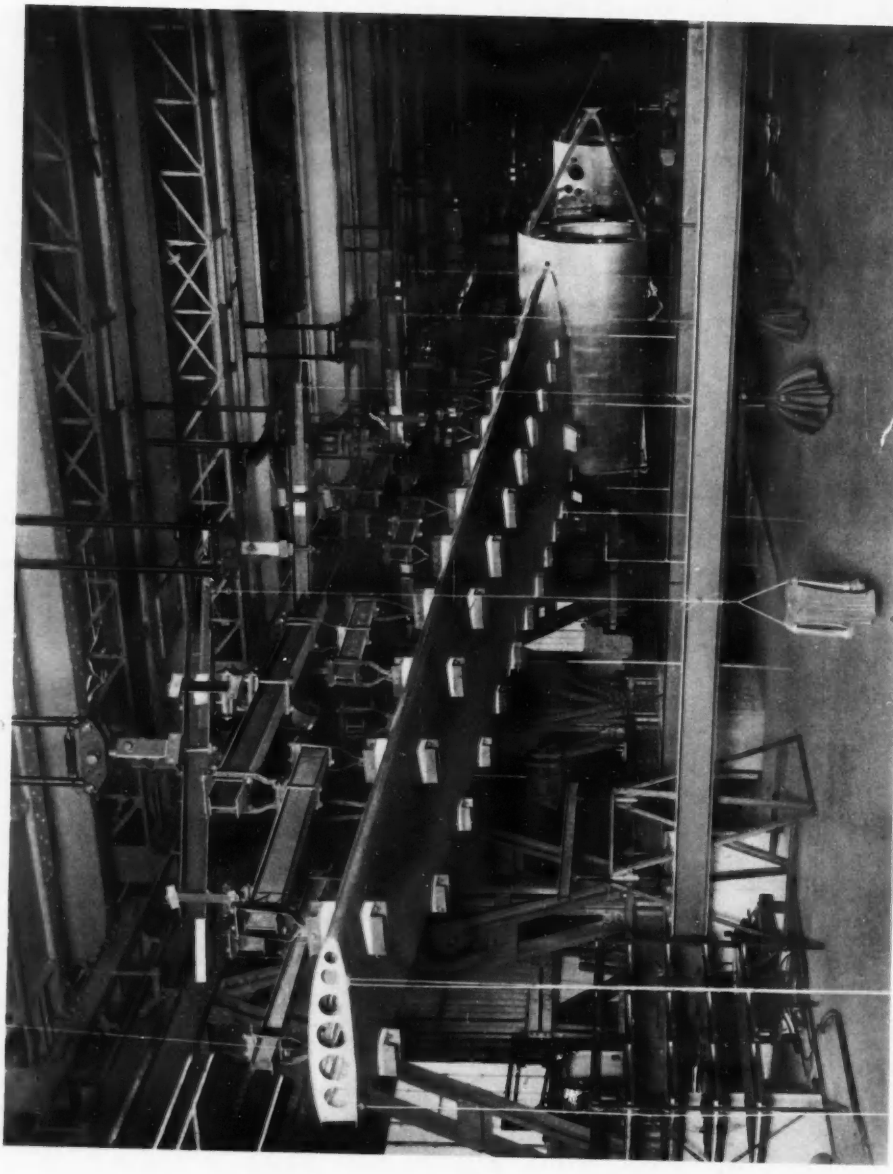

STRUCTURE TESTING AT THE ROYAL AIRCRAFT ESTAB'SHMENT, FARNBOROUGH.

[*Crown copyright reserved. Reproduced by permission of H.M. Stationery Office.*

An article on this subject appears in this issue.

An article on this subject appears in this issue.

Koepe Winders

By A. B. PRICE, B.Sc., A.M.I.Mech.E.
Fraser & Chalmers Engineering Works.

In the Ruhr Coalfield of Germany, the Koepe system of winding has been adopted almost exclusively. Most Continental coal-mining engineers have shown a marked preference for this type of winder, but in British practice the drum winder has been preferred.

In recent years, the National Coal Board has considered the merits of Koepe winding for deep shafts, especially where the system of "horizon" mining is contemplated, and several winders of this type have been ordered. The article deals with the theory and design of the Koepe wheel and should prove useful to all who may be concerned with this system.

WHILE Koepe winders have been used for a great number of years on the Continent, particularly in the Ruhr Coalfield, they have not found favour in this country; there are but few examples to be met with, and these only small winders.

Probably the reason that they are almost exclusively used in Germany is due mainly to the fact that the coal seams are steeply inclined and the "horizon" method of mining is adopted.

Coal lying nearest to the surface is generally worked first and subsequently other and deeper levels are developed. As a result of this method the coal winding levels increase in depth at intervals during the working life of the seams. Sometimes coal is brought to two levels in the one shaft, which is equipped with two winding engines, each fitted with two cages or two skips.

It will be seen that it is advisable to install winders capable of raising heavy loads from the projected deepest levels.

Winders equipped with parallel drums with balance ropes or with a bi-cylindroconical drum are, in many cases, suitable for raising heavy loads from a deep level, though it may mean multi-coiling and very large B.C.C. drums. The drum would, of course, have to be designed to suit the final conditions and may be comparatively too large and uneconomical when winding from the shallower levels. This naturally depends on the difference in depths of the initial and final levels.

Again, if multi-deck cages are used with a B.C.C. drum it is essential to have multiple loading platforms with the necessary loading and unloading equipment.

The Koepe winder can be installed to suit the final conditions of load and depth and, as and when the load increases, it is only necessary to replace the main winding and balance ropes, and adjust the depth indicator and other controls.

The use of keps is not recommended with Koepe winders, and adjustable cage loading platforms or ramps are provided so that cages can be unloaded and loaded while they are suspended from the winding rope.

This is of utmost importance when winding multi-deck cages from deep levels, when the alteration in the length of the winding rope during the decking operation would make the use of keps almost impossible, and certainly undesirable.

In recent years the Koepe system of winding has been more extensively considered in this country especially for deeper shafts and where "horizon" mining is being used. It is felt therefore that the following observations may prove of service to engineers who are interested in the Koepe system of winding.

The system consists essentially of a grooved pulley (figs. 1 and 2), the groove consisting of a special material having a high coefficient of friction so as to reduce rope slip to a minimum. A single rope is used, each end of which is attached to a cage or skip, and passes over the Koepe wheel, the arc of contact depending on the layout adopted. The winding rope is balanced by means of a tail rope, the ends of which are attached to the underside of the cage or skip.

Typical layouts are shown in the following illustrations:

Fig. 3 shows a headgear having the sheaves side by side, and the winder on ground

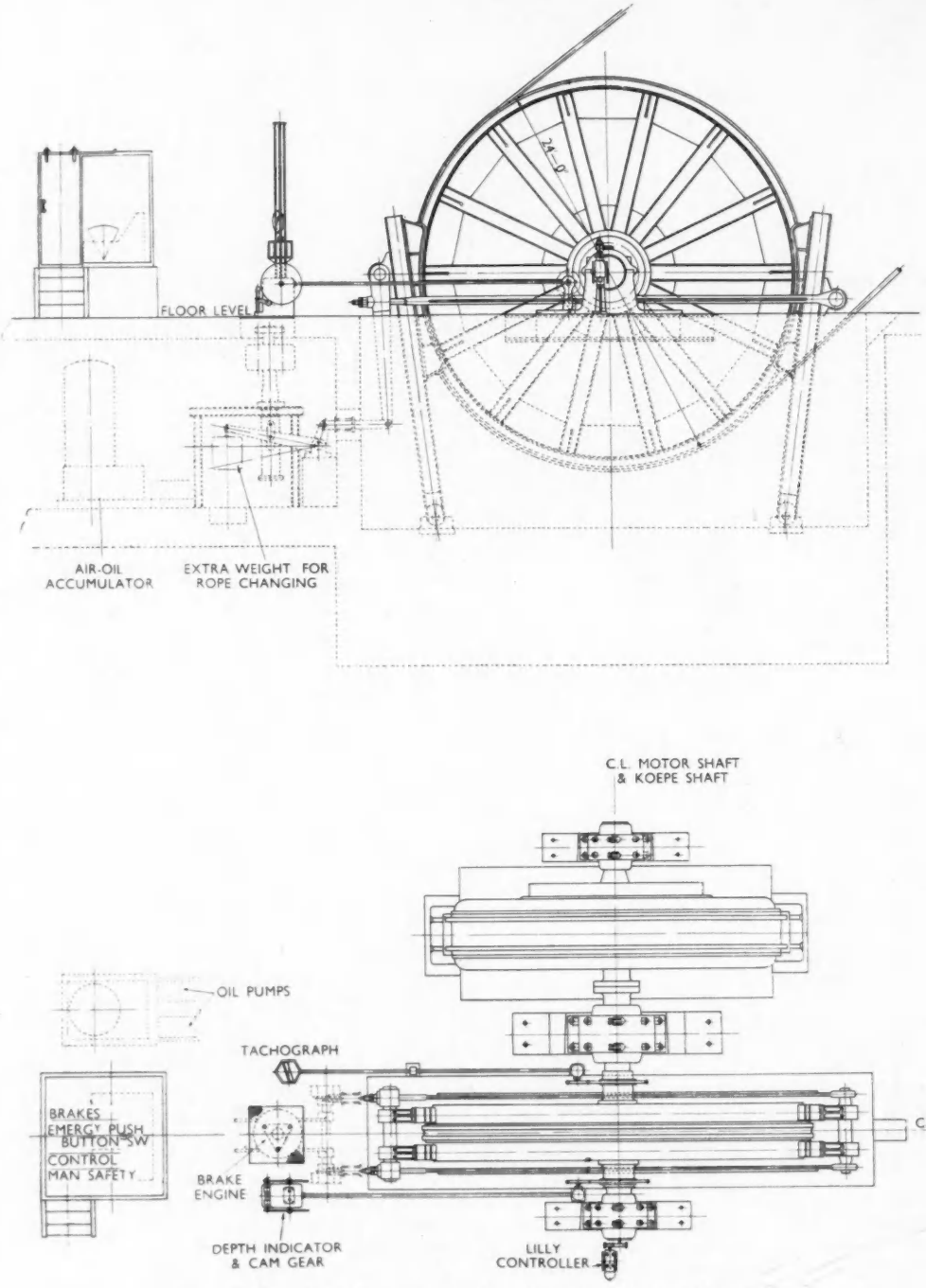

Fig. 1.—Typical arrangement of a motor-driven Koepe pulley winder.

level. With this arrangement the winder must be sufficiently far away from the pit to ensure that the angle α is not more than $1\frac{1}{2}°$ and preferably 1° or less.

Fig. 4 shows a head gear having the sheaves one above the other and in the same vertical plane, the Koepe wheel being in the same plane.

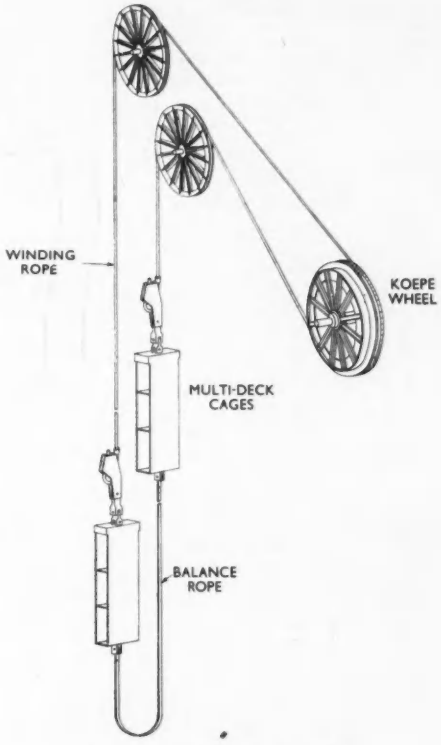

Fig. 2.—Koepe system of winding.

Fig. 5. This arrangement is similar to fig. 4 but has two winders operating on the same shaft. An illustration of such a headgear is shown in fig. 6.

Fig. 7. It will be seen that this is a further development of fig. 5, the difference being that the winder is as near the headgear as possible, so that one rope is vertical or nearly so. This is known as the Mommertz-Lintz system and the advantages claimed are that there is a reduction in shaft pillar area and that as the ropes rise nearly vertically to the head sheaves, fatigue in the wires due to rope sag and oscillation is minimised.

Fig. 8. This is known as the tower type, and there may be either one or two winders accommodated in the engine room carried on the tower, the height to engine room floor being in the neighbourhood of 160 ft.

The arrangement to be adopted naturally depends on local and winding conditions.

FUNDAMENTAL PRINCIPLES.

The Koepe system is applicable to those cases where there is no possibility of rope slip, and the tendency to slip is least when the difference between the tensions with which the rope is strained over the wheel is small in comparison with the smaller of the two tensions in the rope. In order to make this difference as small as possible the use of a tail or balance rope is desirable and, in deep shafts, imperative.

Generally, for minimum slip, the ratio of the nett load lifted to the total load suspended on the heavier side of the Koepe sheave should not exceed 30 per cent.

The rates of acceleration and retardation are carefully controlled as they affect the pull on the rope. In practice the acceleration is kept to a minimum and should not exceed 3·28 ft./sec./sec.

To guard against slipping of the rope on the Koepe wheel the ratio of the pulls on the ascending or descending portions of the ropes under the worst conditions of loading must not exceed an amount determined by the angle of contact and the coefficient of friction.

Consider fig. 9 :

Let P and p = tensions with which the rope is strained over the pulley, P being greater than p.

θ = arc of contact in radians.

μ = coefficient of friction between the rope and the lagging.

e = Napierian base = 2·7183.

When the rope is on the point of slipping in a direction from p towards P

$$P = pe^{\mu\theta}$$

$$\text{or } \frac{P}{p} = e^{\mu\theta}$$

$$\text{or } log\frac{P}{p} = 0{\cdot}4343\mu\theta$$

Thus if on a Koepe wheel the angle of contact is 210° or $(210 \times 0{\cdot}0175) = 3{\cdot}67$ radians and the coefficient of friction is 0·2, slipping will take place when the ratio of the rope pulls on the two sides exceeds 2·09.

The worst condition is at the start of the wind when the pull on the ascending rope is the sum of the full cage, rope and pull due to acceleration. On the descending rope the pull is equal to the empty cage, plus balance rope minus acceleration pull.

In designing Koepe wheels one method is to ascertain the maximum permissible acceleration and retardation and make sure that the running conditions are such that this acceleration and retardation are not exceeded.

The three conditions which require consideration are:

(1) Lifting the load at the start of the wind (fig. 10)

(2) Braking at the end of the wind when lifting load (fig. 11)

(3) Lowering a load and braking (fig. 12).

(1) Lifting the load at the start of the wind (fig. 10)

Let T_1 = load on the ascending rope = wts. of rope + cage + trams + coal.

T_2 = load on descending rope = wts. of balance rope + cage + trams.

G = weight of each sheave referred to rope centre + wt. of ropes between Koepe wheel and head sheave, i.e. = $(H + R_3)$ in fig. 10.

$$M_1 = \frac{C + L + R_1 + H + R_3}{g} = \frac{T_1}{g} + \frac{G}{g}$$

$$M_2 = \frac{C + R_2 + H + R_3}{g} = \frac{T_2}{g} + \frac{G}{g}$$

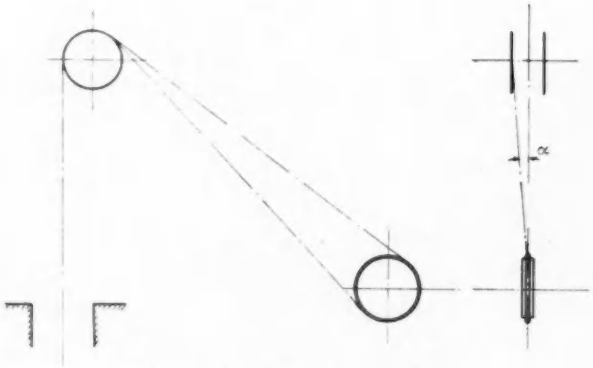

Fig. 3.—Diagram showing rope leads.

a = acceleration in ft./sec./sec.

r = retardation in ft./sec./sec.

F = friction.

Then $$P = T_1 + \frac{T_1 a}{g} + \frac{Ga}{g} + F = T_1 + (T_1 + G)\frac{a}{g} + F$$

$$p = T_2 - \frac{T_2 a}{g} - \frac{Ga}{g} - F = T_2 - (T_2 + G)\frac{a}{g} - F$$

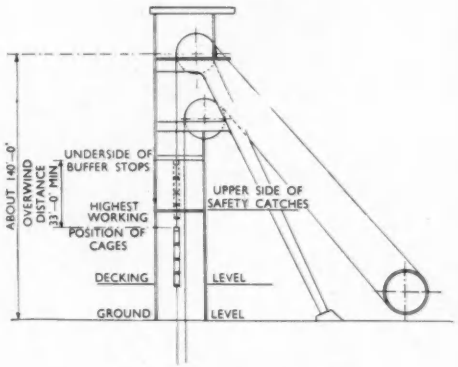

Fig. 4.—Arrangement of pithead frame.

When rope slip begins

$$\frac{P}{p} = e^{\mu\theta}$$

i.e. when $$e^{\mu\theta} = \frac{T_1 + (T_1 + G)\frac{a}{g} + F}{T_2 - (T_2 + G)\frac{a}{g} - F} = \frac{T_1 g + (T_1 + G)a + Fg}{T_2 g - (T_2 + G)a - Fg}$$

from which expression we get the maximum acceleration

$$a = \frac{e^{\mu\theta}(T_2 - F) - (T_1 + F)}{e^{\mu\theta}(T_2 + G) + (T_1 + G)} \times g$$

(2) Maximum retardation permissible when braking with a lifting load (fig. 11)

$$P = T_1 - \frac{T_1}{g} r - \frac{G}{g} r + F$$

$$p = T_2 + \frac{T_2}{g} r + \frac{G}{g} r - F$$

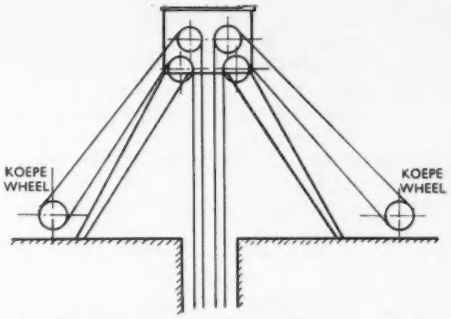

Fig. 5.—Diagram of head frame for 4-cage shaft.

Slipping starts when $\frac{p}{P} = e^{\mu\theta}$

so that maximum permissible retardation

$$r = \frac{e^{\mu\theta}\,(T_1 + F) - (T_2 - F)}{e^{\mu\theta}\,(T_1 + G) + (T_2 + G)} \times g$$

(3) Maximum retardation permissible when braking with a lowering load (fig. 12)

$$P = T_1 + \frac{T_1}{g}R + \frac{G}{g}R - F$$

$$p = T_2 - \frac{T_2}{g}R - \frac{G}{g}R + F$$

so that maximum permissible retardation

$$R = \frac{e^{\mu\theta}\,(T_2 + F) - (T_1 - F)}{e^{\mu\theta}\,(T_2 + G) + (T_1 + G)} \times g$$

When calculating the above retardations it is usual to ignore friction F, as this allows a margin of safety, since any friction assists braking.

Another method of calculating safety against slip factor is as follows :

Consider fig. 13 :

T_1 = Tension in the rope carrying the useful load = wts. of rope + cage + trams + coal.

T_2 = Tension in the unloaded rope = wts. of rope + cage + trams.

P = actual pull on the rope due to T_1 and also to acceleration (or retardation) and friction.

p = pull on the rope due to T_2 and also to acceleration (or retardation) and friction.

Slipping will not take place if $P \gtreqless pe^{\mu\theta}$

If S = actual moving force
$= P - p$

S_{max} = maximum moving force which will not cause slip.
= maximum permissible tension in the rope carrying the useful load − tension in the unloaded side.
$= P_{max} - p$
$= pe^{\mu\theta} - p$

Fig. 6.—An installation in the Ruhr showing typical head frame for 4-cage shaft.

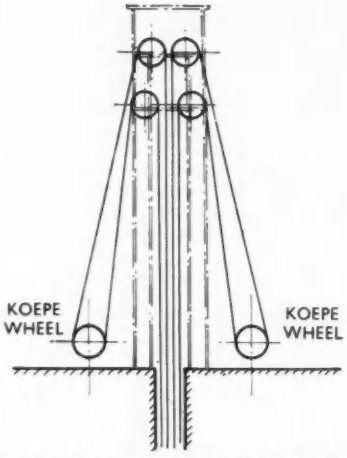

Fig. 7.—Alternative design of head frame for 4-cage shaft (Mommertz Lintz system).

$$\left.\begin{matrix}\text{Factor of safety}\\ \text{against rope slip}\end{matrix}\right\} = \gamma = \frac{S_{max}}{S}$$

$$\gamma = \frac{P_{max} - p}{P - p} = \frac{pe^{\mu\theta} - p}{P - p}$$

$$= \frac{p\,(e^{\mu\theta} - 1)}{P - p}$$

(1) Consider lifting the load at the start of the wind (fig. 10).

As before :

L = useful load in lbs.

C = weight of cage bridles, etc. + empty trams in lbs.

R_1 = weight of rope suspended on the loaded side.

R_2 = weight of rope suspended on the unloaded side.

R_3 = weight of rope between Koepe wheel and head sheave.

H = weight of head sheave referred to rope centre.

G = weight of each sheave referred to rope centre + weight of rope between Koepe wheel and head sheave, i.e. $(H + R_3)$ in fig. 10.

a = acceleration in ft./sec./sec.

r = retardation in ft./sec./sec.

F = friction.

$T_1 = C + L + R_1$

$T_2 = C + R_2$

$$P = T_1 + \frac{T_1}{g}a + \frac{G}{g}a + F$$

$$= (C+L+R_1) + \left(\frac{C+L+R_1}{g}\right)a + \left(\frac{H+R_3}{g}\right)a + F$$

$$= (C+L+R_1)\left(1 + \frac{a}{g}\right) + (H+R_3)\frac{a}{g} + F$$

$$p = T_2 - \frac{T_2}{g}a - \frac{G}{g}a - F$$

$$= (C+R_2) - \left(\frac{C+R_2}{g}\right)a - \left(\frac{H+R_3}{g}\right)a - F$$

$$= (C+R_2)\left(1 - \frac{a}{g}\right) - (H+R_3)\frac{a}{g} - F$$

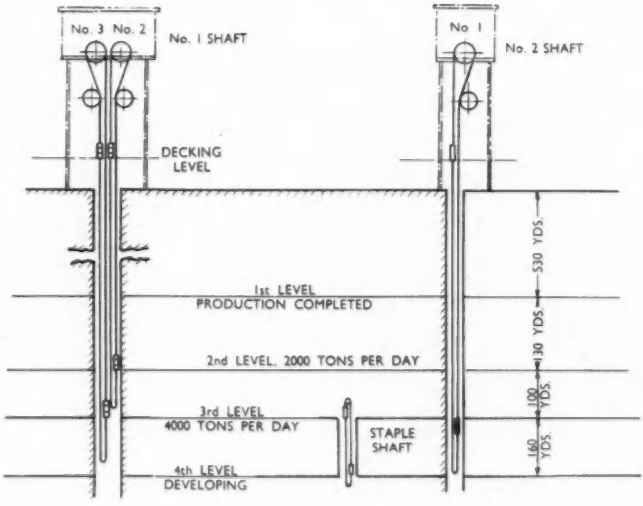

Fig. 8.—Arrangement of Tower type head frame.

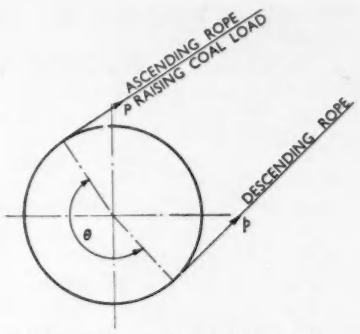

Fig. 9.—Forces acting on Koepe pulley.

$$\text{Safety factor} = \frac{p\,(e^{\mu\theta}-1)}{(P-p)}$$

(2) Braking at end of wind when lifting load (fig. 11)

$$P = T_1 - \frac{T_1}{g}r - \frac{G}{g}r + F$$

$$= (C+L+R_1) - \left(\frac{C+L+R_1}{g}\right)r - \frac{(H+R_3)}{g}r + F$$

$$= (C+L+R_1)\left(1-\frac{r}{g}\right) - \frac{G}{g}r + F$$

$$p = T_2 + \frac{T_2}{g}r + \frac{G}{g}r - F$$

$$= (C+R_2) + \left(\frac{C+R_2}{g}\right)r + \left(\frac{H+R_3}{g}\right)r - F$$

$$= (C+R_2)\left(1+\frac{r}{g}\right) + \frac{G}{g}r - F.$$

In this case slipping will not take place if :

$$= p \lessgtr Pe^{\mu\theta}$$

$$\text{Safety factor } S_R = \frac{P\,(e^{\mu\theta}-1)}{p-P}$$

(3) Safety against rope slip when winding at constant speed and lifting the load :

$$\text{Safety factor} = \frac{(C + R_2 - F)\,(e^{\mu\theta} - 1)}{L + 2F}$$

(4) Lowering the load and applying the brake (fig. 12) :

$$P = T_1 + \frac{T_1}{g}r + \frac{G}{g}r - F$$

$$= (C+L+R_1) + \left(\frac{C+L+R_1}{g}\right)r + \left(\frac{H+R_3}{g}\right)r - F$$

$$= (C+L+R_1)\left(1+\frac{r}{g}\right) + (H+R_3)\frac{r}{g} - F.$$

$$p = T_2 - \frac{T_2}{g}r - \frac{G}{g}r + F$$

$$= (C+R_2) - \left(\frac{C+R_2}{g}\right)r - \left(\frac{H+R_3}{g}\right)r + F.$$

$$= (C+R_2)\left(1-\frac{r}{g}\right) - (H+R_3)\frac{r}{g} + F.$$

$$\text{Safety factor} = \frac{p\,(e^{\mu\theta}-1)}{P-p}$$

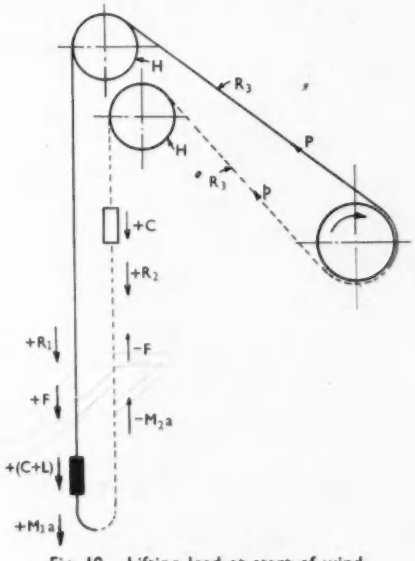

Fig. 10.—Lifting load at start of wind.

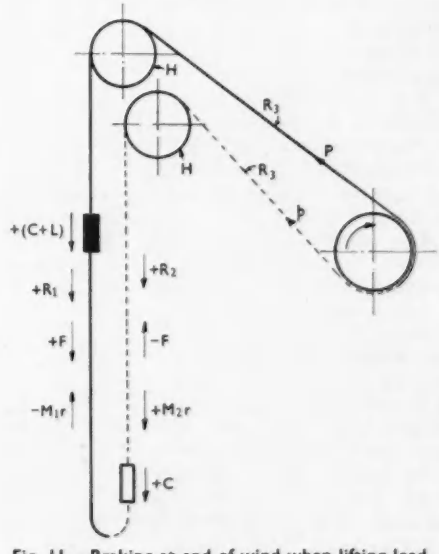

Fig. 11.—Braking at end of wind when lifting load.

It will be seen that the diameter of the Koepe wheel does not enter into any of the above calculations and has, therefore, theoretically no influence on the rope slip. The rope pressure on the lagging, however, may affect the coefficient of friction and alter the value $e^{\mu\theta}$, and

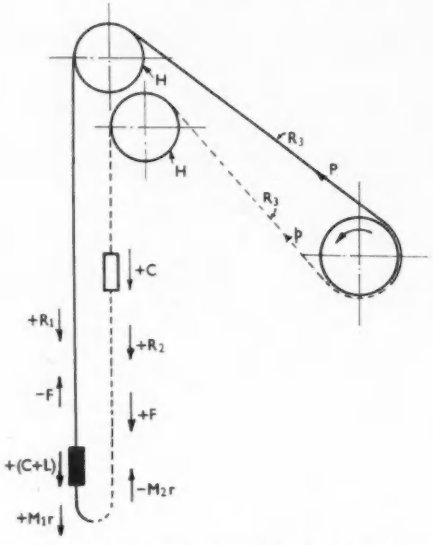

Fig. 12.—Braking and lowering at end of wind.

this specific surface pressure is, of course, dependent on the wheel diameter. The influence, which is not very considerable, depends upon the alteration of form of the lagging groove under rope pressure.

The decisive factors are the unbalanced load relative to the balanced loads, which may increase or decrease the possibility of rope slip according to whether it is descending or ascending, and the rates of retardation or acceleration, as the case may be.

The effective load which can be raised or lowered, the rate of acceleration or retardation, are dependent on the total load suspended, the arc of contact and the coefficient of friction. This coefficient is governed by the type of lagging adopted, and the type and condition of the winding rope. In order to increase the coefficient of friction, ropes are often treated with a special lacquer paint which tends to keep the rope dry and grease from working out of it.

As already stated the rate of acceleration should not exceed 3·28 ft./sec./sec., while the maximum rope speed should not exceed :

(*a*) 65 ft./sec. when winding material.

(*b*) 40 ft./sec. when winding and lowering persons.

These speeds are, however, subject to new regulations which are, at the moment, under consideration.

KOEPE WHEEL.

The driving wheels of a Koepe winder are constructed according to several different designs, viz. :

(1) Cast steel.

(2) Cast steel or cast iron hub with steel arms and rim of riveted construction. Such a wheel is indicated in fig. 14 which shows a half of the pulley in the manufacturer's works.

(3) Cast steel hub with channel steel arms and rim of welded construction. An idea of this design of wheel may be obtained by referring to fig. 15; the pulley is 23 ft. diameter, designed to lift a 12 ton useful load from a depth of 640 yds. and is directly coupled to a 2,200 h.p. motor.

There are two types of driving wheels, the general construction being indicated in figs. 16 and 17. The design adopted depends on the method to be used for rope changing. In the case of the design shown in fig. 16 a special winch has to be used for this purpose, but in the other design (fig. 17) the wheel is so constructed that the whole length of rope can be wound on and accommodated on the wheel.

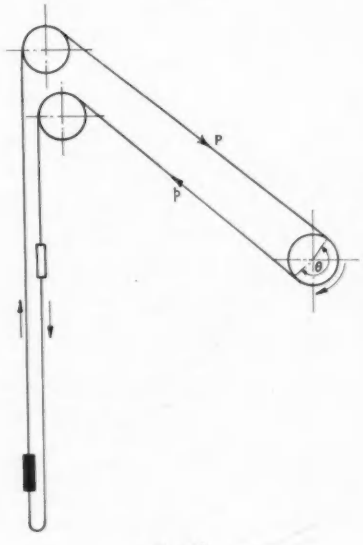

Fig. 13.

Fig. 14.—Koepe wheel, riveted construction.

The two methods for changing ropes are described later.

The diameter of the wheel is decided by the diameter of the rope, and the specific pressure of the rope on the lagging.

Generally, the diameter of the wheel is between 100 to 120 times the diameter of the rope, whilst the rope pressure is arranged to be between 180 and 230 lbs./sq. in. This pressure is given by the equation :

$$P = \frac{L}{D \times d}$$

where P = rope pressure in lbs./sq. in.

Fig. 15.—Koepe wheel of welded construction, 23 ft. diameter, nett load 12 tons, depth of wind 640 yards.

D = diameter at the bottom of the groove in inches.
d = rope diameter in inches.
L = total suspended load on both ropes, in lbs.

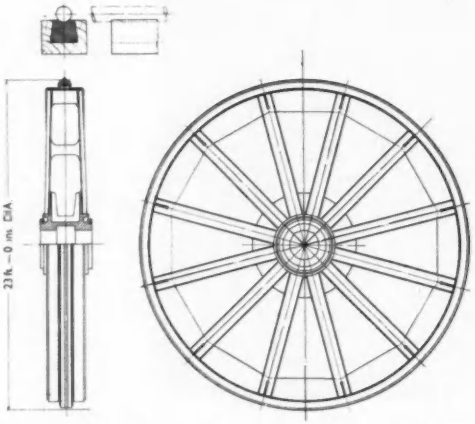

Fig. 16.—Koepe wheel of welded construction without rope magazine.

In order to increase the coefficient of friction between the rope and the lagging, several types of material are being used. The lagging itself usually consists of inserts securely fixed in wood blocks, which are in turn bolted to the rim of the wheel. The blocks are made in different designs, some being solid with a groove cut out to take the inserts, while others are in two or three pieces suitably bolted together.

Many materials are used for the inserts, perhaps the most common being leather. When this is used, two kinds are cemented together alternately, one consisting of a hard hide and the other of a tough chrome leather.

Many winders are fitted with "Ferodo" inserts, and in some cases old rubber conveyor belt has been suitably cut and fitted into the wood blocks. Experiments have been carried out in Germany with inserts made of an aluminium alloy, but so far with doubtful success. On some of the smaller winders plain wood blocks, usually of elm, are fitted.

The coefficient of friction varies according to the material used, and is roughly as follows :

	At rest :	*Slipping :*
Plain wood blocks	0·35	0·20
Leather	0·45	0·22
"Ferodo"	0·45	0·22
Aluminium alloy	0·5	0·23

It will be noted that when the rope is at rest relative to the lagging the coefficient of friction is reasonably good; but when slip has begun this coefficient is considerably reduced.

For calculation and design purposes, a coefficient of friction of 0·2 is taken which it will be seen is only just a little less than the figures given in the table when the rope has started to slip.

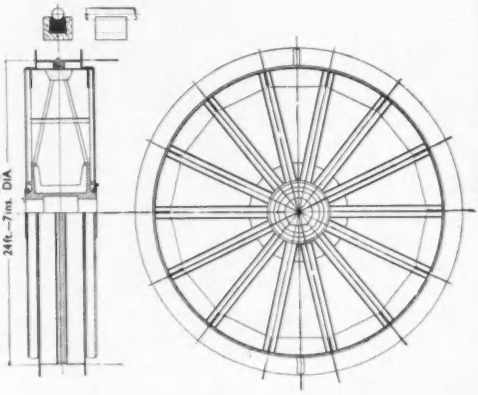

Fig. 17.—Koepe wheel of welded construction with rope magazine.

If the Koepe system is properly designed and maintained, the possibility of rope slip is slight because the design is based on a coefficient of friction which is less than the actual static coefficient of friction. It is apparent that it is most important to ensure that the designed load, rates of acceleration and retardation are not exceeded, and that the winding rope and friction lining are kept free from excessive moisture and grease.

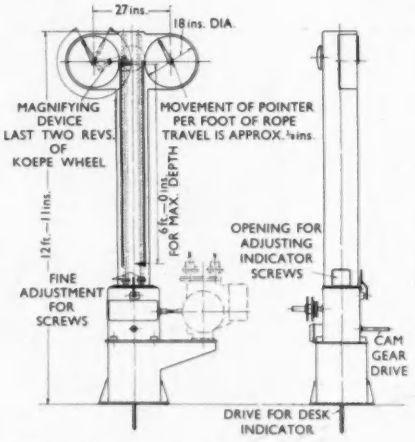
27ins.
18ins. DIA.
MAGNIFYING DEVICE LAST TWO REVS. OF KOEPE WHEEL
MOVEMENT OF POINTER PER FOOT OF ROPE TRAVEL IS APPROX. ½ins.
12ft.-11ins.
6ft.-0ins. FOR MAX. DEPTH
OPENING FOR ADJUSTING INDICATOR SCREWS
FINE ADJUSTMENT FOR SCREWS
CAM GEAR DRIVE
DRIVE FOR DESK INDICATOR

Fig. 18.—Vertical screw depth indicator.

The Koepe wheel is driven either directly by a slow speed motor or through a set of reduction gears by a high-speed machine. In nearly all cases to date the Ward-Leonard system of control is used, especially for winders driven

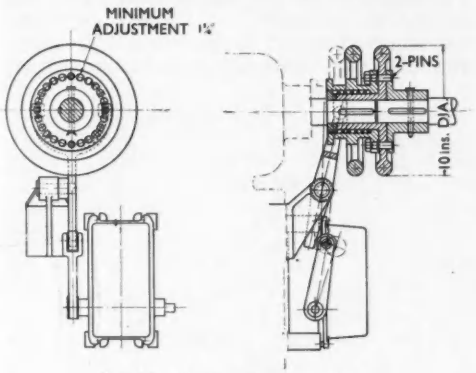

Fig. 19.—Vernier type coupling.

by motors of about 1,000 h.p. and over. The D.C. Ward-Leonard winder is preferred because of its simple and flexible method of speed control and the ease with which adequate safety devices can be incorporated.

Depth Indicator.

Several types of depth indicators can be used, but probably the most popular is what is known as the " vertical screw type ". This consists of two screws each carrying a nut with a pointer, which indicates the position of the cage on a suitable scale, the length of which is about 6 ft. For deep winds, the ratio of the depth of the shaft to the length of the scale of the overwinder can be very high. To reduce this ratio at the beginning and end of the wind, a dial indicator is introduced which only comes into operation some 200 ft. from the end of the wind and acts as a magnifying device. Such a depth indicator is shown in fig. 18.

The indicator is positively driven from the Koepe wheel shaft by suitable gearing, and a " Lilly " controller can also be driven from the same drive.

Rope creep occurs with every Koepe winder when there is difference between the loads in each cage, and in normal winding this can amount to about 18 ins. in a normal shift of some 8 hours. This creep affects the setting of the control gear and other protective devices, which are driven from the Koepe wheel shaft, and it is, therefore, necessary to make adjustments from time to time. For this purpose a Vernier type coupling, similar to that shown in fig. 19, is introduced in the shaft driving the depth indicator and near to the indicator itself. Further, each screw of the indicator can be adjusted independently. It will be noticed that a switch is incorporated so that when the coupling is disconnected the brakes are automatically applied.

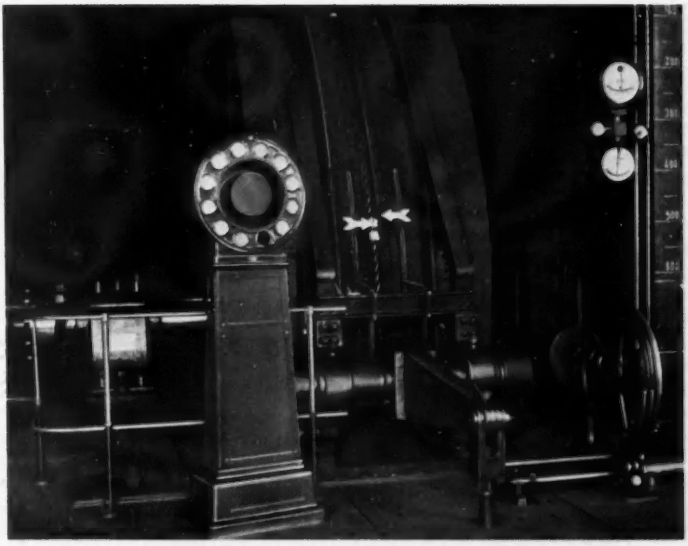

Fig. 20.—Koepe wheel 24 ft. 7 ins. diameter, showing rope markings.

For finally bringing the cages to bank, marks are painted on the cheeks of the drums in the case of drum winders. This, of course, is impracticable with Koepe winders, and it is usual to mark the rope itself, each mark corresponding to a deck of the cage. Such marks are clearly indicated in fig. 20.

D.C. electric winders are usually fitted with cam control gear, which limits the rate of acceleration and the maximum speed, and ensures a maximum rate of retardation by controlling the movement of the driver's lever during mineral and man winding.

The cams are either fitted to the depth indicator itself or consist of a separate item, and are driven by a suitable shaft and gearing. The cams can be arranged so that they turn more slowly during the constant speed portion of the wind, but increase in speed during the acceleration and retardation periods, thus increasing sensitivity of control during these periods.

A "Lilly" controller is incorporated in the control gear, and its function is so well known that further comments are unnecessary.

The depth indicator is also fitted with overwind switches, these switches being operated slightly after those on the "Lilly" controller. The effectiveness of these switches, however, is dependent on the absence of slip between the rope and the Koepe wheel. As a safeguard against the danger of rope slip, these switches are backed up by installing overwind switches in the headframe which are operated by the cages.

Brakes.

The usual type of brakes fitted to Koepe winders is shown in fig. 1. They can be operated by any design of efficient brake engine, and should be capable of fulfilling certain conditions which are now being considered by the Ministry of Fuel and Power.

Pending these new regulations coming into force, it will be of interest to refer to those covered by the German regulations.

These state that every winding engine with a man-winding speed of more than 13·1 ft./sec. must be provided with two brakes, namely a service brake and an emergency brake. The service brake must be fitted with a suitable regulator, so that its braking effort corresponds to the position of the driver's brake lever. Also, the regulator must be fitted with a pressure gauge showing the effective pressure in the brake cylinder. The emergency brake must operate the same brake shoes as the service brake, but it must be independent of energy supplied to the winder. Emergency brakes, which are weight operated, must be so arranged that no momentum can be caused by the weight falling, and they must come into action as quickly as possible.

Both brakes must be independently capable of holding the winding engine with the maximum unbalanced load with a static factor of safety of at least three. Further, under like conditions the service brake must be capable of producing a retardation of at least 6·56 ft./sec./sec.

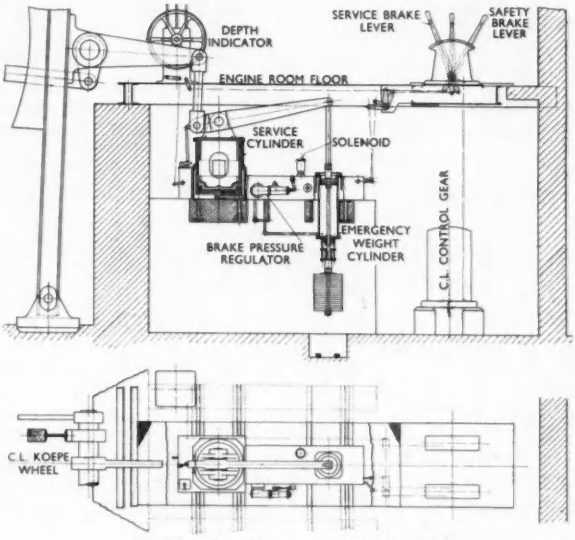

Fig. 21.—Quick-acting air brake engine.

When determining the power of the brakes a coefficient of friction of 0·4 must be used for smooth turned brake paths, while for unturned paths the figure is 0·3. In the static and dynamic calculations of the brakes, no account must be taken of additional braking forces (such as shaft and mechanical friction).

The static factor of safety of at least 3 applies to the emergency brake of Koepe winders for main shafts, provided the rope slip limit based on a coefficient of friction of 0·2 between the rope and lagging is not exceeded.

The mechanical strength of the brake gear must be such that it ensures a factor of safety of at least 5 with respect to the maximum working brake-force. This brake-force is usually that exerted by the service brake, taking into account the maximum air pressure in the brake cylinder.

In unusual cases, such as when an overwind occurs, both brakes may be operated simultaneously, but during normal winding this should be avoided if the total brake pressure exceeds the greatest normal pressure of the service brake. Fig 21 shows a typical brake gear arrangement, which is very popular in Germany. This quick acting service and emergency brake engine is operated by compressed air, and consists of a service brake cylinder controlled by a brake pressure regulator (fig. 21a) and a holding cylinder for the brake weight. The two brake cylinders are connected by a floating lever, which is also linked up to the main brake lever operating the four brake posts.

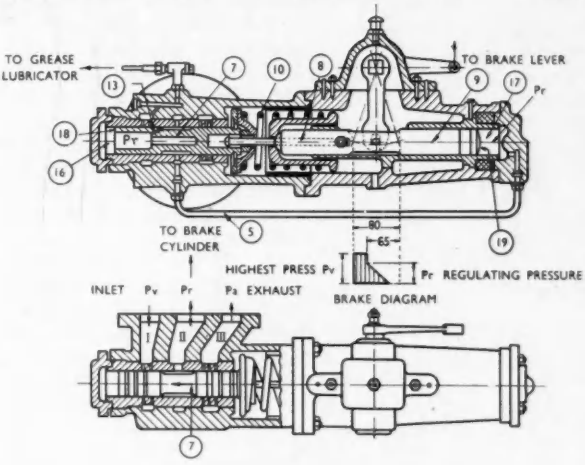

Fig. 21a.—Brake pressure regulator.

When used as a service brake it is controlled by the driver's service brake lever, which operates the pressure regulator, so that the air pressure is proportional to the movement and position of the lever. Air pressure is admitted to the underside of the piston of the emergency or weight cylinder, and thus the weight is held in its top position, and is therefore out of action.

The brakes are normally applied by admitting air pressure to the underside of the service brake piston. This lifts the floating lever which turns about a fulcrum above the weight cylinder, thus applying the brakes.

The brake pressure regulator enables the driver to apply any desired brake pressure up to a predetermined maximum, and he can, therefore, avoid too great a braking effort which might cause rope slip.

The maximum air pressure which can be applied is controlled by adjusting the regulator so that the brake will hold the winder with a static factor of safety of 3, and produce a minimum retardation of 6·56 ft./sec./sec. when lowering the usual unbalanced load. The air pressure is usually of the order of 60 lbs. per sq. in.

In the case of an emergency, the brake can be applied in about 0·25 seconds after tripping by de-energising the brake solenoid which causes the regulator to admit compressed air to the " service " cylinder, and at the same time open a valve which releases air from the weight cylinder. The service cylinder has a short stroke, about 1¼ ins. to 2 ins., and the brakes are applied before air has had time to exhaust from the weight cylinder, so that the weight is held in position by the service cylinder. There is no momentum effect due to the weight, because it does not fall unless the air pressure drops to that value which is required to produce the lowest permissible braking effort.

Should this occur the safety brake is applied by a minimum air pressure device, which operates so that the service cylinder applies the brakes, but the weight falls slowly until the pressure in the service cylinder balances the pressure due to the weight.

As the " safety brake " can be applied automatically, it must be adjusted so that rope slip cannot occur ; but it is desirable, after stopping the winder, that its braking effort should be equal to the maximum brake-force of the service brake. The maximum permissible rate of retardation which can be applied without causing rope slip is determined by the formulae given earlier, and the travel of the air pressure regulator is adjusted by a limiting device so that the air pressure applied will produce the required rate of deceleration.

With this design the winder is stopped by a braking force which will not cause the rope to slip, but when it has come to rest the braking effort is increased to the desired maximum by the brake weight which falls slowly. The brake weight is such that it will produce the same braking effort as the service brake.

An adjustable throttle valve is introduced in the exhaust pipe of the weight cylinder in order to prevent premature action of the weight during the full speed portion of the wind. The action of this valve is cut out shortly before the end of the wind by a suitable cam fitted to the depth indicator, i.e. when the speed of the winder is considerably reduced. From this point, therefore, the brake acts with full force for safety

against overwinding, and brings the winder to rest, and holds it so, with the same effort as the service brake.

The throttle valve is always full open when the service piston is in its lowest position in its cylinder, i.e. in the " brake off " position. The

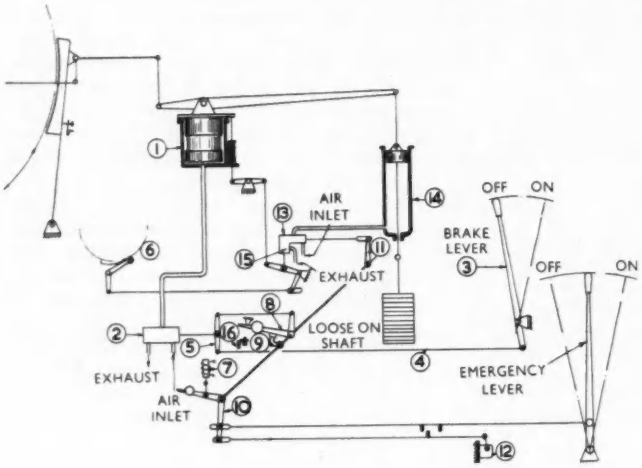

Fig. 22.—Diagram of brake control gear.

throttling action only becomes effective when the piston moves upwards into the " brake on " position. This prevents any delay in the action of the brake weight when the safety brake is applied, if, for any reason, the piston in the service cylinder should not move into the " brake on " position.

Should both the service and emergency levers be pulled simultaneously, the brake is applied with a force only equal to that of either the " service brake " or of the " safety brake ". Combined action of the service and safety brakes cannot occur, so that excessive retardation, and thus rope slip, are avoided.

The control, service brake and emergency brake levers are so interlocked that the safety brake cannot be taken " off " after it has been automatically applied until the service brake lever has been drawn into the " brake on " position and the control or power lever into the " off " position.

Further, the service brake lever and the control lever are interlocked so that power cannot be supplied to the motor when the service brake is applied.

Mention has been made of the brake pressure regulator shown in fig. 21a and the action of this is as follows :

The regulator is shown in the brake's " half on " position, and consists essentially of a piston valve (7), piston (9) and spring (10). To increase the braking effort piston (9) is moved towards the left by means of the two levers shown. This piston, through spring (10), moves piston valve (7) to the left, thus connecting port I to port II, the latter admitting compressed air to the brake engine service cylinder.

Port II is connected to chamber (16) by port (13) and to chamber (17) by balance pipe (5), so that both chambers are under the same air pressure, *Pr*, as the brake engine cylinder. Pressure *Pr* acts on equal areas (18) and (19) of the piston valve (7) and piston (9) respectively.

The air pressure on valve face (18) exceeds the force of the spring and pushes the piston valve back to its original mid-position.

The force of the spring acting on piston (9) will be compensated by the increased pressure *Pr* acting on face (19), so that the gear is again in equilibrium.

To take the brakes " off " piston (9) is moved towards the right. Piston valve (7) then follows this piston, and port II is connected to port III and so to exhaust, and the brakes are released. The air pressure acting on faces (18) and (19) is also reduced, so that the spring forces the piston valve back to its mid-position.

Normally the stroke of piston (9) is adjusted to travel about 2·56 ins. and so permits the air pressure to reach a predetermined value. By increasing the stroke to the maximum (about 3·15 ins.) the highest air pressure available can be admitted to the brake cylinder and the braking effort increased to its maximum. Usually the regulator is adjusted to the shorter stroke, while the full stroke is only brought into use in exceptional circumstances, such as for installing ropes.

As long as the air supply to the regulator is equal to or greater than the maximum adjustable pressure of the regulator, the braking power corresponding to the position of the brake lever is constant and is independent of the air pressure of the supply. It is customary to have the compressed air supply somewhat higher than the maximum pressure to which the regulator can be adjusted.

A diagrammatic sketch of the control gear is shown in fig. 22, and a pictorial drawing in fig. 22a. The service brake is operated by hand by the driver pulling brake lever (3), rod (4) and oscillating lever (5) which operates the pressure regulator (2) by rotating about its upper point.

The application of the brake in case of emergency is effected as follows :

(1) At will, by the engine driver pulling the emergency brake lever.

(2) Automatically, by electrical gear and through safety devices incorporated in the circuit of the brake solenoid (7).

On the main shaft are levers (8), (9), (10) and (11), lever (8) being loose on, and levers (9), (10) and (11) rigid with the shaft. Lever (8) is supported by lever (9). Levers (8) and (10) each carry a weight which when the safety brake, i.e. the brake weight, is lifted, are kept in a raised position by solenoid (7) acting on (10).

The application of the safety brake is always effected by de-energising solenoid (7), even when the brake is applied with the emergency brake lever, since in such a case the solenoid circuit is broken by switch (12).

If the solenoid circuit is broken by switch (12) or by some other device, weight lever (10) is freed. The shaft rotates, levers (9) and (11) turning with it. Lever (9) frees weight lever (8) which operates the brake pressure regulator, the oscillating lever (5) then turning about its lower point, while lever (11) changes the position of piston valve (13). The compressed air in the supporting cylinder (14) is released through the adjustable throttle valve (15). The emergency brake weight is freed. The brake blocks are, however, in contact with the brake paths due to the action of the service brake (1) to which air has already been admitted by regulator (2), so that the brake weight cannot drop and remains suspended. (16) is a regulating stop which decides the fall of the lever (8) and so the travel of brake pressure regulator (2). If (16) has been so adjusted as to give a lower braking effort by the service brake than by the emergency brake weight, then the weight gradually falls.

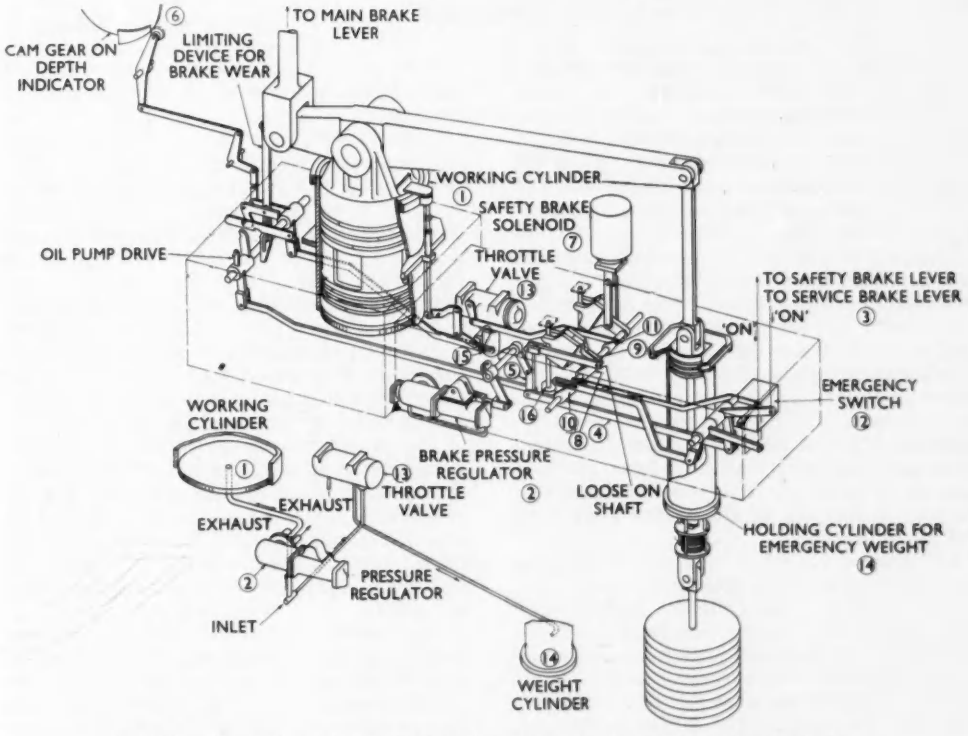

Fig. 22a.—Schematic arrangement of quick-acting air brake engines and control gear.

If the service brake is already applied when solenoid (7) is de-energised, the brake pressure regulator having already been operated via oscillating lever (5) which in this case would have turned about its upper point, then weight lever (8) remains suspended, while weight lever (10) performs its movement and changes the position of piston valve (13).

If, when the mechanism is in this state the brake lever is for any reason brought into the " off " position, then the oscillating lever (5) turns about its centre, and the weight lever (8) follows this movement, and so holds the pressure regulator in its original position.

This process is carried out in the reverse order, viz. should the safety brake be applied and the brake lever put into the " on " position.

Although the solenoid drops rapidly and unfailingly when its circuit is broken, care has to be taken to ensure that the piston valve (13) can also be operated direct by the emergency lever. If, for some reason, the solenoid does not drop when the circuit is broken, then the driver has the means of using the emergency lever, which is connected to lever (10) by a slotted rod, to turn the shaft direct and operate piston valve (13) and regulator (2).

The lifting of the safety brake, i.e. the weight, is effected by placing the emergency lever in the " off " position. Owing to an interlocking device this cannot be done until the brake lever has been put in the " on " position so that when the safety brake is lifted, the brake blocks are kept in contact by the service brake. This ensures that the brake effort is not diminished when the safety brake is lifted. Further interlocking devices are adopted to ensure that before the safety brake is lifted the control lever must be placed in its neutral position.

Similarly, as a result of this interlocking gear, the service brake cannot be released until the safety brake lever has been returned to its neutral position. Were it not for this interlocking gear, it would be possible to release the service brake, and the winder would be started up without the safety brake having been previously placed in the neutral position, so that the automatic release of the safety brake would then fail.

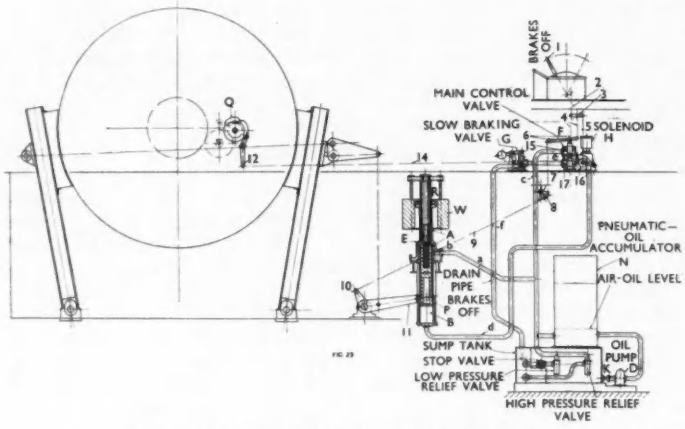

Fig. 23.—Fraser & Chalmers oil-operated brake engine.

A pressure-operated braking engine has been developed by Fraser and Chalmers Engineering Works, and the principle is shown in fig. 23. The engine *E* consists of a two-diameter cylinder, the smaller diameter being at *A* and the larger at *B*. Working in this cylinder are two pistons, namely piston *R* carrying the brake weight *W* and a lower piston *P* which has two different diameters.

Pressure oil is provided by the geared pump *D* through pipe *a* and enters the engine by port *b*, thus tending to force the two pistons *P* and *R* apart. Due to the movement of piston *R* the weight *W* travels upwards until a stop is reached, while piston *P* is controlled by introducing balanced oil pressure at *B*, the oil being supplied by the pump through pipes *a*, *c*, control valve *F* and pipe *d*.

As the oil pressure is the same at each end of the piston *P* it is forced upwards, due to the greater area at its lower end, until it reaches the lower part of the weight piston *R*.

The oil supply from the pump *D* is also connected to the air/oil receiver *N*. In operation, the receiver is pre-charged with air of equal pressure to that of the oil, so that the oil level is just above the inlet and outlet pipes. Thus the receiver acts as a pneumatic-oil accumulator, and ensures rapid and smooth application of the brakes.

The brakes are shown in the " off " position and are applied by movement of the lever (1) towards the right. This action depresses rod (2) and through the floating lever (3) rod (4) and control valve *F*. This movement allows oil to pass from under piston *P* through pipe *d*,

passing from port (16) of the valve *F* to port (17) and thence via pipe *e*, valve *G* and the pipe *f* to the oil sump tank.

The release of pressure from under the piston *P* allows the pressure at the top side of the piston

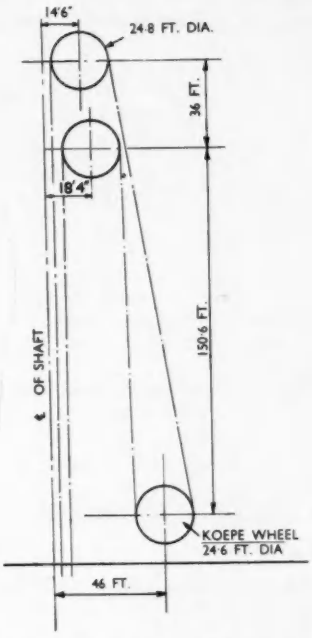

Fig. 24.—Relative position of Koepe wheel and head sheaves.

to force this piston downwards and thus apply the brakes.

To ensure that the position of the brakes corresponds to that of the brake lever, a "follow up" gear is fitted consisting of the lever (10), rod (9), lever (8), rod (7) and floating lever (6).

To release the brakes, the brake lever (1) is moved back to its original position to the left, this action operating the main valve *F* connecting port (15) to (16). This allows oil to flow to the underside of piston *P* through pipes *a*, *c* and *d*, and due to the diameter of the piston at *B* being greater than at *A*, the piston is forced upwards and thus releases the brakes.

In the event of an emergency trip, or current failure, the solenoid *H* connected to the control valve *F* falls and through the rod (5), floating lever (3), rod (4) and the lever (6) moves the piston valve in *F* in a downward direction, allowing oil to pass from under *B* and thus apply the brakes.

In order to control the rate of application of the brakes during the full speed part of the wind, a slow braking valve *G* is introduced into the system, and is operated by a cam *Q* through lever (12) and rod (14).

The cam ensures the valve ports being fully open during the acceleration and deceleration periods of the wind, but the oil flow is partially restricted to a predetermined rate of flow during the intermediate full speed portion of the wind.

In the event of the oil pressure failing, weight *W* moves downwards and applies the brakes.

The braking effort depends on the oil pressure so that it can be controlled by regulating this pressure. This is done by incorporating a suitable relief valve in the system, which can be adjusted to any desired oil pressure.

It will be seen that the application of the brakes depends on oil pressure only and, in an emergency, the rate of application is independent of the inertia of the brake weight.

Load Diagrams for Koepe Winders.

These are calculated in much the same way as for a cylindrical drum winder working with a balance rope, and the resultant diagram resembles that for a drum winder.

With Ward-Leonard control, however, it is possible to arrange for the acceleration to be graded, i.e. the rate of acceleration is constant for a certain portion of the acceleration period, and is then gradually reduced to zero during the remaining portion of that period, the reduction in rate following a parabolic curve. It will be found that the peak horsepower is considerably lower than in the case of constant acceleration throughout the period, but the size of the winder motor and the units of electric power consumed per wind are practically the same for both conditions of acceleration.

Consider the following example of an actual plant installed. The winding conditions are as follows :

Output per hour	535 tons.
Depth of wind	3444 ft.
Coal raised per wind	13·76 tons.
Weight of cage, bridles, etc.	13·1 tons.
Weight of each car	1·57 tons.
Capacity of each car	3·44 tons.
Decks per cage	2.
Cars per cage	4.
Winding rope diameter	3·15 ins.
Winding rope weight per foot	16·3 lbs.
Balance rope weight per foot	16·3 lbs.
Diameter of Koepe wheel	24·6 ft.
Relative positions of Koepe wheel and head sheaves	Fig. 24.

Inertia of Koepe wheel $\left(\frac{WR^2}{g}\right)$ 162500 lbs. ft.^{2}

Head sheave diameter 24·8 ft.

Inertia of head sheave $\left(\frac{WR^2}{g}\right)$ 38000 lbs. ft.^{2}

Inertia of motor rotor $\left(\frac{WR^2}{g}\right)$ 143000 lbs. ft.^{2}

Pressure on lagging $=$

$$\frac{\text{Total suspended load on both ropes.}}{\text{Diam. at bottom of groove} \times \text{rope diam.}}$$

Suspended load :		
coal		30800 lbs.
2 cages		58600 lbs.
8 cars		28160 lbs.
2 ropes		121000 lbs.
(each 3710 ft.)		
		238560 lbs.

Pressure $=$

$$\frac{238560}{[(24{\cdot}6 \times 12)-3] \times 3{\cdot}15} = 260 \text{ lbs./sq. in.}$$

Angle of contact $= 190^\circ \times 0{\cdot}0175 = 3{\cdot}33$ radians.
Coefficient of friction between rope and lagging to be taken as 0·2.

$$\log \frac{P}{p} = 0{\cdot}4343 \times 0{\cdot}2 \times 3{\cdot}33$$
$$= 0{\cdot}289$$
$$\therefore \frac{P}{p} = 1{\cdot}945 = e^{\mu\theta}$$

Safety against rope slip:

	T_1	T_2
Coal	30800 lbs.	— lbs.
Cage	29300	29300
4 trams	14080	14080
3710 ft. rope	60500	60500
	134680	103880

G = weight of each head sheave referred to rope centre + weight of rope between pulley and head sheave

$$= \frac{38000 \times g}{(12{\cdot}4)^2} + 2500 = 11100 \text{ lbs.}$$

F = friction $= 0{\cdot}06$ coal load.
$= 0{\cdot}06 \times 30800 = 1850$ lbs.

Maximum permissible acceleration at start of wind:

$$a = \frac{e^{\mu\theta}(T_2 - F) - (T_1 + F)}{e^{\mu\theta}(T_2 + G) + (T_1 + G)} \times g$$
$$= \frac{1{\cdot}945\,(103880-1850)-(134680+1850)}{1{\cdot}945\,(103880+11100)+(34680+11100)} \times g$$
$$= 5{\cdot}4 \text{ ft./sec./sec.}$$

Maximum retardation permissible at end of wind when lifting the load:

$$r = \frac{e^{\mu\theta}(T_1+F)-(T_2-F)}{e^{\mu\theta}(T_1+G)+(T_2+G)} \times g$$

When calculating retardation it is usual to ignore friction F. This allows a margin of safety, since any friction assists braking.

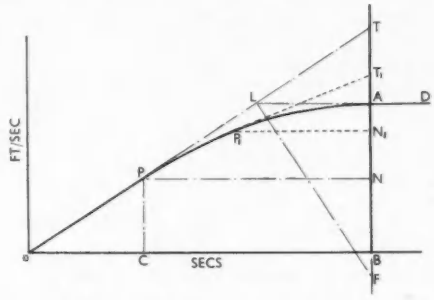

Fig. 25.—Graded acceleration diagram.

$$r = \frac{(1{\cdot}945 \times 134680)-103880}{1{\cdot}945\,(134680+11100)+(103880+11100)} \times g$$
$$= 12{\cdot}7 \text{ ft./sec./sec.}$$

Maximum retardation permissible when braking with a lowering load:

$$R = \frac{e^{\mu\theta}(T_2+F)-(T_1-F)}{e^{\mu\theta}(T_2+G)+(T_1+G)} \times g$$

again ignoring friction.

$$R = \frac{(1{\cdot}945 \times 103880)-134680}{1{\cdot}945\,(103880+11100)+(134680+11100)} \times g$$
$$= 5.86 \text{ ft./sec./sec.}$$

$$\text{Winds/hour} = \frac{\text{tons per hour}}{\text{tons per wind}} = \frac{535}{13{\cdot}76} = 39$$

$$\text{Time of cycle} = \frac{3600}{39} = 92{\cdot}5 \text{ secs.}$$

Decking time is taken as $8 + 4 + 8 = 20$ secs.
Winding time 72·5 secs.

Usually, the times of acceleration and retardation are estimated from experience, but, in this case, the winder is arranged to run at maximum permissible speed, viz. 65·6 ft./sec. and the constant acceleration is taken as 3·28 ft./sec./sec. which is below the maximum permissible, viz. 5·40 ft./sec./sec.

Assume total acceleration time = 30 secs.
Refer to fig. 25.
Horizontal scale 1 cm. = 2 secs.
Vertical scale 1 cm. = 10 ft./sec.
OB = 30 secs. = 15 cms.
BT = 3·28 ft./sec./sec. × 30 secs. = 98·4 ft./sec.
= 9·84 cm.

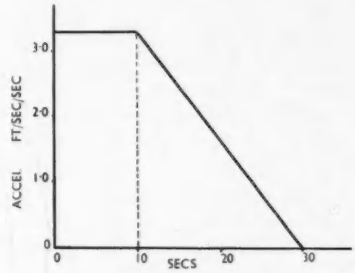

Fig. 26.—Acceleration-time diagram.

Maximum rope speed = 65·6 ft./sec.
$\therefore$ BA = 65·6 ft./sec. = 6.56 cm.
Draw the parabola having OT and AD as tangents.
The characteristic of the parabola is such that $AT = AN$
i.e. $AN = BT - AB$
= 98.4 − 65·5 = 32·8 ft./sec. (3·28 cm.)
$PC = AB - AN$ = 65·6 − 32·8 = 32·8 ft./s. (3·28 cm.)

$$\therefore \quad OC = \frac{\text{Velocity}}{\text{accel.}} = \frac{32{\cdot}8}{3{\cdot}28} = 10 \text{ secs.}$$

$\therefore$ graded acceleration time = 30 − 10 = 20 secs.

$$AL = \tfrac{1}{2}\, PN = 5 \text{ cm.}$$

$$\frac{AF}{AL} = \frac{AL}{AT}$$

$$AF = \frac{AL^2}{AT} = \frac{5^2}{3{\cdot}28} \text{cm.} = 7{\cdot}62 \text{cm.}$$

Equation for the parabola is $y = \dfrac{x^2}{4a}$

Where a = 7·62 cm.

i.e. $y = \dfrac{x^2}{30{\cdot}48}$ cm.

Acceleration at any point $P_1 = \dfrac{T_1N_1}{P_1N_1} = \dfrac{2AN_1}{P_1N_1}$

$$\therefore \quad \text{acceleration } f = \frac{2 \times 10y \text{ ft./sec.}}{2x \quad \text{secs.}}$$

$$= \frac{10y}{x} \text{ ft./sec./sec.}$$

Radial acceleration a =

$$\frac{f}{\text{radius of wheel}} = \frac{f}{12{\cdot}3} \text{ rad./sec./sec.}$$

It will be seen from fig. 26 that if the acceleration is plotted against the time, a straight line results.

Moments of Inertia. $\left(I = \dfrac{WR^2}{g} \text{ lbs. ft.}^2\right)$

Koepe wheel	162500 lbs. ft.²
Head sheaves referred to Koepe shaft	75000 lbs. ft.²
Motor rotor	143000 lbs. ft.²
	380500 lbs. ft.²

Coal	30800 lbs.
2 cages	58600 lbs.
8 cars	28160 lbs.
2 ropes	121000 lbs.

$$\frac{WR^2}{g} = 238560 \times \frac{12{\cdot}3^2}{g} = 1120000 \text{ lbs. ft.}^2$$

$\therefore$ total value of I = 1500500 lbs. ft.²

Mean static torque =
30800 × 12·3 = 379000 ft. lbs.

Allow overall efficiency of 85 per cent.

$$\text{Friction} = 379000 \times \left(\frac{100}{85} - 1\right)$$

$$= 379000 \times 0{\cdot}18$$

$$= 66000 \text{ ft. lbs.}$$

$$T_M = 379000 + 66000 = 445000 \text{ ft. lbs.}$$

Table 1 (fig. 27) can now be prepared as follows:
Velocity at any point v = 65·6 − 10y ft./sec.

$$RPM = \frac{v \times 60}{\text{wheel circ.}} = \frac{60v}{\pi \times 24{\cdot}6}$$

$$\text{Now } \lambda = \frac{2\pi \times RPM}{33000} = \frac{2\pi}{33000} \times \frac{60v}{\pi \times 24{\cdot}6} = \frac{v}{6765}$$

T_A = Total inertia × radial acceleration
$= I \times a$

$HP = (T_M + T_A)\,\lambda$

$$\text{Max. } RPM = \frac{60 \times 65{\cdot}6}{\pi \times 24{\cdot}6} = 51$$

To find times of constant speed and retardation, from fig. 25.

Distance travelled during acceleration :
= Area under curve.
$= \frac{1}{2}\,(OC \times PC) + (PN \times PC) + \frac{2}{3}\,(AN \times PN)$
$= \frac{1}{2}\,(10 \times 32{\cdot}8) + (20 \times 32{\cdot}8) + \frac{2}{3}\,(32{\cdot}8 \times 20)$
= 1257 ft.

$\therefore$ distance travelled during constant speed and retardation = 3444 − 1257
= 2187 ft.

Let r = time of retardation

$$\text{Rope speed} = 65{\cdot}6 = \frac{2187}{72{\cdot}5 - 30 - \frac{r}{2}} \text{ ft./sec.}$$

Whence $r = 18{\cdot}2$ secs.

$\therefore$ constant speed period $= 42{\cdot}5 - 18{\cdot}2 = 24.3$ sec.

$$\text{Retardation} = \frac{51\ RPM \times 2\pi}{60 \times 18{\cdot}2} = 0{\cdot}294 \text{ rad./sec./sec.}$$

$$\text{Retardation torque} = I \times 0{\cdot}294 = 15005000 \times 0{\cdot}294 = 440000 \text{ ft. lbs.}$$

$$\text{Net torque during retardation period} = T_M - 440000 = 445000 - 440000 = 5000 \text{ ft. lbs.}$$

$$HP = \frac{5000 \times 2\pi \times 51\ RPM}{33000} = 48.7$$

Curves shown in figs. 28 and 29 can now be prepared.

Units per wind (Winder only).

H.P. secs. = Area of diagram fig. 29.

$$= \left(\frac{4100}{2} \times 10\right) + \left(\frac{4100 + 4650}{2}\right)2 + \left(\frac{4650 + 5100}{2}\right)2 + \text{etc.} + \left(\frac{4690 + 4320}{2}\right)2 + (4320 \times 24{\cdot}3) + (48{\cdot}7 \times 18{\cdot}2) = 227526$$

$$\text{Units/wind} = \frac{227526 \times 0{\cdot}746}{3600 \times 0{\cdot}92} = 51{\cdot}2$$

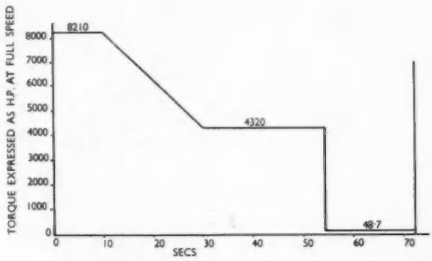

Fig. 28.—Horsepower-time diagram.

RMS Rating of Winder Motor, from fig. 28 :

$$RMS = \sqrt{\frac{(8210^2 \times 10) + [8210^2 + 4320^2 + (8210 \times 4320)]\frac{20}{3} + (4320^2 \times 24{\cdot}3) + (48{\cdot}7^2 \times 18.2)}{(\frac{1}{2} \times 30) + 24{\cdot}3 + (\frac{1}{2} \times 18{\cdot}2) + (\frac{1}{3} \times 20)}}$$

$= 5900 + 5$ per cent (say) $= 6200$ h.p.

TABLE 1.

Time	$t = x$	y cm.	$10y$ ft./sec.	v ft./sec.	f ft./sec.^{2}	a rad./sec.^{2}	$T_A = I \times a$	$T_A + T_M$	λ	H.P.
10	10	3·28	32·8	32·8	3·28	0·267	400,000	845,000	0·00486	4100
12	9	2·65	26·5	39·1	2·94	0·239	358,000	803,000	0·0058	4650
14	8	2·1	21·0	44·6	2·63	0·214	321,000	766,000	0·0066	5100
16	7	1·605	16·05	49·55	2·29	0·186	279,000	724,000	0·00734	5310
18	6	1·18	11·8	53·8	1·97	0·1605	241,000	686,000	0·00797	5470
20	5	0·82	8·2	57·4	1·64	0·133	200,000	645,000	0·0085	5480
22	4	0·525	5·25	60·35	1·31	0·1065	163,000	608,000	0·00892	5420
24	3	0·295	2·95	62·65	0·985	0·08	120,000	565,000	0·00927	5240
26	2	0·131	1·31	64·29	0·655	0·0532	80,000	525,000	0·00953	5000
28	1	0·033	0·33	65·27	0·33	0·0267	40,000	485,000	0·00966	4690
30	0	0	0	65·6	0	0	0	445,000	0·00972	4320

Fig. 27.

Stresses in Koepe Wheel.

Each designer has his own methods of determining the stresses in the Koepe wheel, but the following particulars, which are accepted by the German Mines Department, will no doubt prove of interest.

Fig. 30 shows the cross section of the Koepe pulley.

The moment of inertia and modulus of section of the area are calculated in the usual way.

Let L = greatest rope pull in lbs.
T_M = maximum torque in inch lbs.
F = Force exerted by one pair of brake posts in lbs.
R = radius of rope centre in ft.

Referring to figs. 30 and 31 :

A = area of section in sq. ins.
I = moment of inertia of section (in.^{4})
Z = modulus of section (in.^{3})
x, y = distances of outer edges from neutral axis (inches)
S = length of arc between two arms in inches.
h = height of this arc in inches.
n = number of arms.
A_2 = area of one pair of arms (in.^{2})
A_3 = area of one diagonal bracing (in.^{2})
l = length of arm in inches.
r = radius of hub in inches.
B = length of brake block in inches.

Rim Plate Stresses.

The greatest stress occurs when the brakes are applied, and is due to the rope pull plus the pressure of the brakes.

The specific pressure on 1 inch length of rim is :

(1) due to rope pull

$$\text{i.e. } P_1 = \frac{L}{12R} \text{ lbs./in.}$$

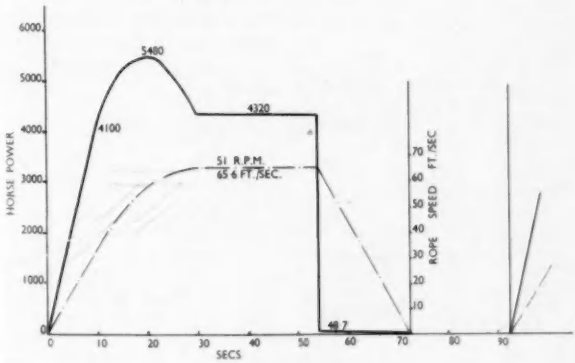

Fig. 29.—Duty cycle.

(2) due to brake pressure

$$\text{i.e. } P_2 = \frac{F}{B} \text{ lbs./in.}$$

$\therefore$ total pressure $= P_1 + P_2 = P$ lbs./in.

Correction coefficient for end thrust :

$$\eta = \frac{1}{1 + \dfrac{45\,I}{4A \times h^2}}$$

The greatest stress occurs at the point where the arms meet the rim.

Reference to the text-book "Hütte", 23rd edition, page 151, will show the rim treated as a bent beam which is assumed to be fitted in the arm connection.

The maximum stress f is exerted on this connection.

$$f = -\frac{\text{Moment } M_A}{\text{Modulus } Z} - \frac{\text{Abutment pressure}}{\text{Section } A_1}$$

$$= -\left(\frac{P \times S^2}{12} \times \frac{1-\eta}{Z}\right) - \left(\frac{P \times S^2}{8h} \times \frac{\eta}{A_1}\right) \text{ lbs./sq.in.}$$

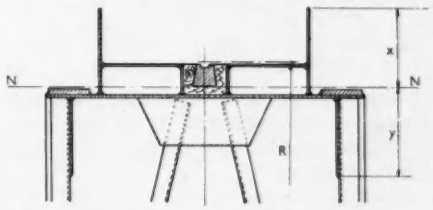

Fig. 30.—Cross section of Koepe pulley rim.

Stress in the Arms.

The greatest stress occurs :

(1) At starting when the arms bend under maximum torque T_M, and are at the same time compressed by the radial force of the rope pull.

According to Bach in his book "Maschinen Elemente" the bending moment :

$$M_3 = \frac{T_M}{l+r} \times \frac{l}{3} \times \frac{2l+3r}{l+2r} \text{ lbs. ins.}$$

If Z_A = total modulus of section of the arms, Stress $f_3 = \dfrac{M_3}{Z_A}$

Neglecting relief due to the rim of the wheel, the pressure on the arms due to rope pull, and assuming the diagonal bracing takes no load :

$P_R = P_1 \times S$ lbs.

Stress $f_R = \dfrac{P_R}{A_2}$

$\therefore$ total stress $= f_3 + f_R$

(2) On account of the application of the brakes, and the radial force of the rope pull:

$$P_3 = S \times (P_1 + P_2) \text{ lbs.}$$

$$f_B = \frac{P_3}{A_2} \text{ lbs./sq. ins.}$$

Stress in the Welds.

The German regulations for the welding of steel structures DIN.4100, 2nd edition, published in July 1933, stipulate under clause 5 that calculations must be based on 0·65 times the ultimate strength of the material.

Stresses in the welded joints are:

(1) Joint between hub plate and arm:
Bending moment according to Bach:

$$M_1 = \frac{T_M}{l_1 + r_1} \times \frac{l_1}{3} \times \frac{2\,l_1 + 3r_1}{l_1 + 2r_1}$$

or in each arm $M_2 = \frac{M_1}{n}$

The polar moment of resistance of the welded joint is:

$$Z_1 = \frac{2}{9} \times \frac{a^3b - a_1^3b_1}{a}$$

$$\text{Stress } f_1 = \frac{M_2}{Z_1} \text{ lbs./sq. ins.}$$

The welds between the channel flanges and the boss are neglected.

(2) Welded joint between the arms and segmental rim plates.
Bending moment:

$$M_3 = \frac{T_M}{l_1 + r_1} \times \frac{l_1}{3} \times \frac{l_1 + 3r_1}{l_1 + 2r_1}$$

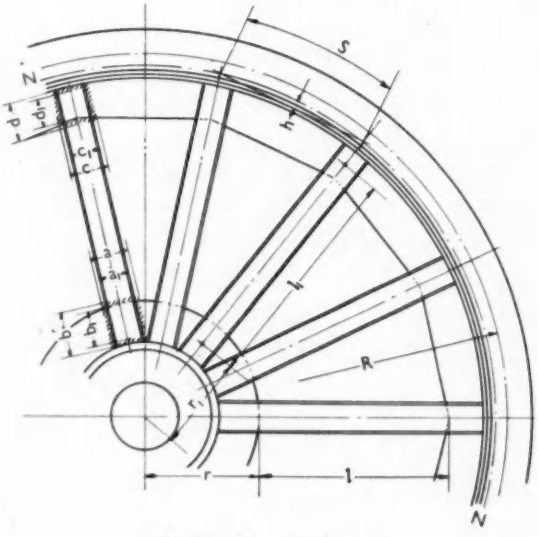

Fig. 31.—Koepe pulley arms.

or in each arm $M_4 = \frac{M_3}{n}$

The polar moment of resistance of the joint is:

$$Z_2 = \frac{2}{9} \times \frac{c^3d - c_1^3d_1}{c}$$

$$\text{Stress } f_2 = \frac{M_4}{Z_2} \text{ lbs./sq. ins.}$$

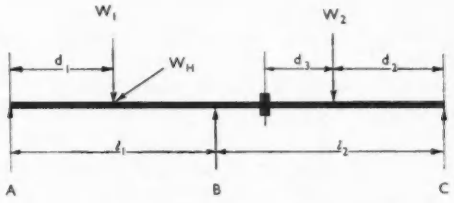

Fig. 32.—Loading of Koepe wheel shaft.

Koepe Wheel Shaft.

Assume a winder direct driven by a D.C. motor.

The forces acting on the shaft are the weights of the Koepe wheel, the motor rotor and the shaft itself, together with the pull of the ropes. This pull is resolved into horizontal and vertical components, and on a ground type winder the vertical component will be upwards, while in the case of a Tower type this component will be downwards.

Referring to fig. 32:

Let W_1 = Weight of Koepe wheel + weight of shaft AB (assumed acting at hub centre) ± vertical component of pull on the ropes.

W_2 = Weight of motor rotor + weight of shaft BC (assumed acting at hub centre).

W_H = Horizontal component of rope pull.

Bending moment due to W_H:

$$M_H = -\frac{W_H}{2\,(l_1 + l_2)} \times \frac{d_1}{l_1}\,(l_1^2 - d_1^2)$$

Horizontal bearing loads are:

Bearing C $\quad C_H = \frac{M_H}{l_2}$

Bearing A $\quad A_H = \frac{[M_H + W_H\,(l_1 - d_1)]}{l_1}$

Bearing B $\quad B_A = \frac{[W_H d_1 - C_H\,(l_1 + l_2)]}{l_1}$

The maximum bending moment due to the vertical components occurs at B and is :

$$M_V = -\left[\frac{W_1}{2(l_1+l_2)} \times \frac{d_1}{l_1}(l_1^2-d_1^2) + \frac{W_2}{2(l_1+l_2)} \times \frac{d_2}{l_2}\left(l_2^2-d_2^2\right)\right]$$

Vertical bearing loads are :

Bearing A $\quad A_V = \dfrac{M_V + W_1(l_1 - d_1)}{l_1}$

Bearing C $\quad C_V = \dfrac{M_V + W_2(l_2 - d_2)}{l_2}$

Bearing B $\quad B_V = \dfrac{W_1 d_1}{l_1} + \dfrac{W_2 d_2}{l_2} - M_V\left(\dfrac{1}{l_1} + \dfrac{1}{l_2}\right)$

From the horizontal and vertical bearing loads the resultant bearing reactions are determined as follows:

Bearing $A = \sqrt{A_H^2 + A_V^2}$

Bearing B $= \sqrt{B_H^2 + B_V^2}$

Bearing C $= \sqrt{C_H^2 + C_V^2}$

The resultant bending moment in bearing $B = \sqrt{M_H^2 + M_V^2} = M_R$

According to Continental practice the equivalent bending moment is obtained as follows :—

If T = maximum torque to which the shaft is subjected

$$q = 0{\cdot}35 + 0{\cdot}65\sqrt{1 + \left(\frac{T}{M_R}\right)^2}$$

Equivalent bending moment

$$M_E = M_R q$$

$$\text{Stress in the shaft} = \frac{M_E}{\text{Modulus of section.}}$$

Stress in Solid Forged Flange Coupling.

The coupling should be designed to take the maximum torque of the motor. In addition to the bolts a diametral key should be fitted between the faces of the two half-couplings.

The bolts should be accurately fitted in reamered holes, and each should have a machined washer.

Referring to fig. 33 :

Let D = outside diameter of flange.
P = pitch circle diameter of bolts.
R = diameter of recess.
W = width of key.
d = diameter of bolts.
n = number of bolts assumed to be 10.
a = cross sectional area of each bolt.
T = maximum torque in inch lbs.

Area of bolts and key subject to shear

$$A = n \times a + (D - R)\,W \text{ sq. ins.}$$

(1) Stress due to torque :

$$f_T = \frac{4}{3} \times \frac{T}{A \times \frac{1}{2}P} \text{ lbs. sq. ins.}$$

(2) Bending moment, refer to figs. 32 and 33 :
Bending moment due to horizontal component.

$$M_H = C_H(d_2 + d_3).$$

and due to vertical component

$$M_V = C_V(d_2 + d_3) - W_2 d_3$$

Resultant bending moment

$$M_R = \sqrt{M_H^2 + M_V^2}$$

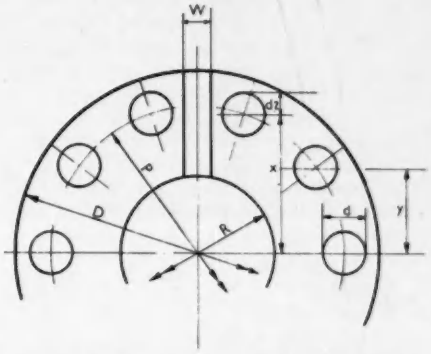

Fig. 33.—Leading dimensions of flange coupling.

The bending moment is resisted by the 10 bolts, and the modulus of these is obtained as follows :

$$\text{Modulus } Z = \frac{2\left[\left(5 \times \frac{\pi d^4}{64}\right) + 2\left(\frac{\pi d^2}{4} \times y^2\right) + 2\left(\frac{\pi d^2}{4} \times x^2\right)\right] \text{in.}^3}{x + \frac{d}{2}}$$

$$\text{Stress } f_B = \frac{M_R}{Z} \text{ lbs./sq. in.}$$

$$\text{Total stress } f = f_B\left[0{\cdot}35 + 0{\cdot}65\sqrt{1 + 4\left(\frac{f_T}{f_B}\right)^2}\right]$$

STAPLE SHAFT WINDERS.

Fig. 8 shows, diagrammatically, the winding arrangements common in the Ruhr Coalfield. Winder No. 1 is used to raise coal from the third level and is employed exclusively for this purpose and in this case winds a skip. No. 2 winder operates between the surface and Nos. 1 and 2 levels, and is used to lower stone to these levels and also to raise coal from No. 2 level. Winder No. 3 is used to lower and raise men or materials from levels 1, 2 and 3, and also coal from No. 3 level in an emergency.

Staple shafts are used for winding between one level and another. For this purpose small drum winders are sometimes used, but more often Koepe winders are installed.

The staple winder is placed in one of three ways :

(*a*) over the shaft, i.e. a similar layout to a tower winder.
(*b*) on the higher level of the staple shaft.
(*c*) on the lower level of the shaft.

The last-mentioned arrangement does not suffer from the effects of subsidence as do the other two methods, and has the advantage of being in intake air. Fig 34 shows the rope and sheave layout in which the Koepe winder is placed under the ladder compartment, and the rope rises in this compartment to sheaves of differing diameters set at an angle to suit the centres of the ropes.

In some instances one cage only is employed, a counterweight being used for balancing. To have equal out-of-balance when raising an empty cage and when raising a cage containing full trams, the counter balance must have a definite weight.

Referring to fig. 35 :

Weight of coal	$L = 8800$ lbs.
Weight of cage, etc.	$C = 6226$
Weight of four trams	$T = 5104$
Weight of rope	$R = 2145$

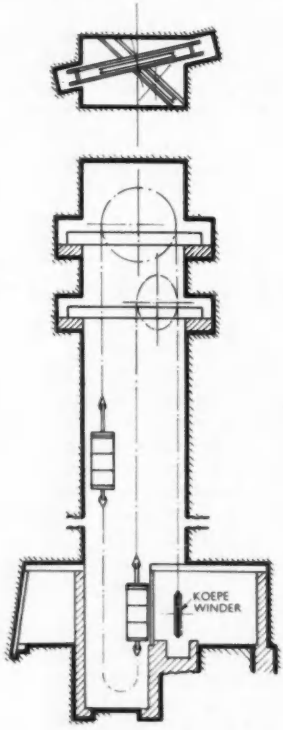

Fig. 34.—Typical arrangement of staple shaft winder.

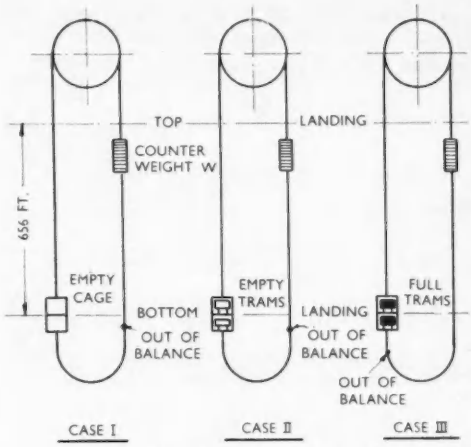

Fig. 35.—Loading of staple shaft winder.

To have equal out-of-balance in cases I and III.

Counterweight $W = \frac{1}{2}(2C+L+T)$
$= \frac{1}{2}(12452+8800+5104)$
$= 13200$ lbs. (say).

Case I. Out-of-balance $= 13200-6226$
$= 6974$ lbs.

Case II. „ $= 13200-(6226+5104)$
$= 1870$ lbs.

Case III. „ $= (6226+8800+5104)-13200$
$= 6930$ lbs.

INSTALLATION OF WINDING AND BALANCE ROPES

Reference has already been made to the two types of Koepe wheels generally used, the design adopted depending on the method used for changing the ropes.

Naturally, each engineer has his own method of dealing with this problem so that the following descriptions should only be considered as typical, and to give an idea of the problems involved.

Koepe Wheel with no Rope Magazine.

In the first case consider the design of wheel shown in fig. 16, i.e. one which has no rope magazine. With this design of wheel it is necessary to have a special rope changing winch, which is driven either by an air-operated reciprocating engine or by a motor.

One type of winch has a cylindrical drum capable of accommodating the whole of the winding rope, and of winding at a speed of about 100 ft./min. The horsepower varies with the depth of the shaft, size of rope and weight of

cage. German engineers take full advantage of the friction between the rope and Koepe wheel when considering the maximum rope pull to which the winch is subjected. It is felt, however, that the brake gear should be strong enough to hold the rope pull resulting from the weights of the cage plus suspended rope.

Sometimes a friction winch is used, and such a machine is illustrated in fig. 36. It will be seen that it consists of two grooved drums geared together, and in this case driven by a duplex air engine.

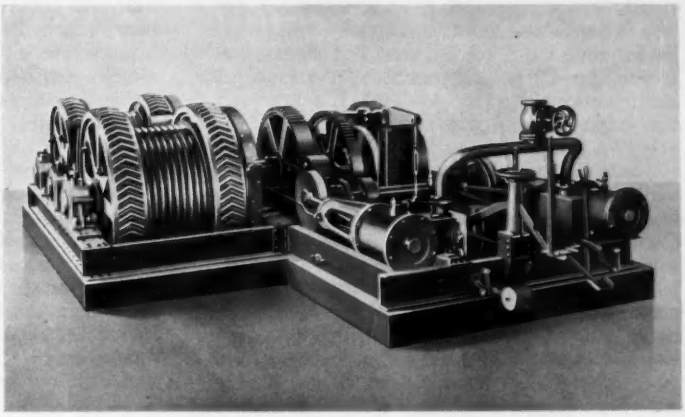

Fig. 36.—Double drum rope changing winch.

Installation of Original Ropes.

Balance Rope.

Refer to fig. 37: a pilot rope is attached to the balance rope which is on the manufacturer's drum *B*, the length of this pilot rope being such that it reaches from the winch *A*, over the guide pulley *D* to pit top, as shown by the dotted line in the diagram.

The pilot and balance ropes are now wound on to the auxiliary winch *A* and a second pilot rope fixed to the other end of the balance rope. It is then threaded over pulley *D* and slowly lowered down the shaft, if necessary using a rider. The

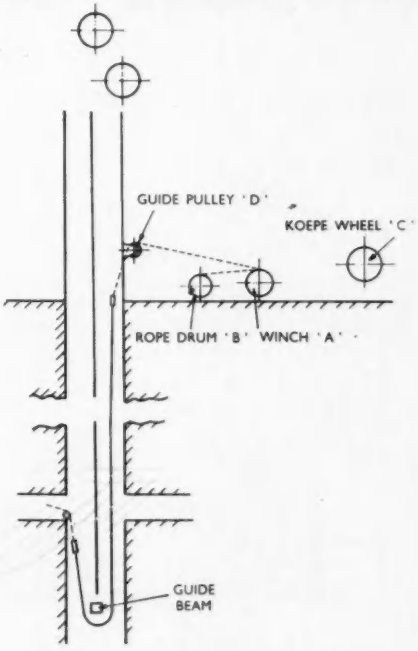

Fig. 37. Installation of ropes.

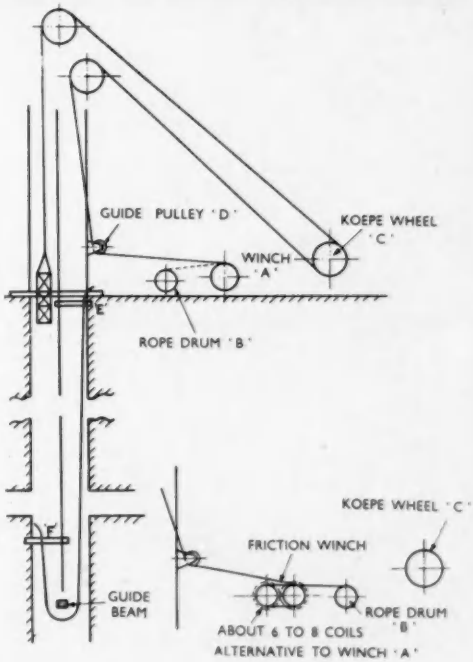

Fig. 38.

speed of lowering is usually between 1·5 and 3·5 ft./sec. The pilot and balance ropes are drawn round the guide beam and clamped as indicated in fig. 38 at *E* and *F*. The pilot ropes are removed.

Winding Rope.

The rope drum *B* (fig. 38) carrying the winding rope is brought into position and a pilot rope is attached, the length of this rope being such that it reaches from winch *A* to pit top. The ropes are then wound from *B* on to winch *A*, when a further pilot rope is attached. By means of this rope the winding rope is threaded under guide pulley *D*, the head sheave, Koepe wheel *C* and over the other head sheave, and attached to the left-hand cage which will already have been placed in position and supported by baulks.

When the rope has been connected up to the cage, the baulks are removed and the cage lowered slowly down the shaft, the winch *A* and Koepe winder turning simultaneously. The rope speed as before should be between 1·5 and 3·5 ft./sec.

On reaching pit bottom, the cage is again supported by baulks, and the other cage placed in position at pit top and also supported by baulks. The rope is clamped at *H* (fig. 39a). The pilot rope is disconnected and the winding rope attached to the right-hand cage. The balance rope is now attached to the cages and the clamps removed.

Fig. 39b shows an alternative method of clamping the ropes, in this case on to the Koepe wheel itself. An idea of a typical clamp is shown in the sketch. The cages must be supported at exactly the correct distance apart when the last attachment is made; but the winding rope should be three to six feet on the short side, according to the depth of the shaft, to allow for the stretching of the rope. Finally, the depth indicators are adjusted, the cages loaded and wound up and down so that initial rope stretch is eliminated, after which the depth indicators are again adjusted.

CHANGING ROPES.

Balance Rope.

The drum *N* carrying the balance rope is taken to pit bottom (fig. 40). The old balance rope is clamped at *P* and *R* and detached from the cages, which are carried on baulks. The new balance rope is connected to the old rope at *S* and a pilot rope at the other end of the old balance rope. Clamps *P* and *R* are released, and the old balance rope is wound on to auxiliary winch *A* pulling the new rope with it.

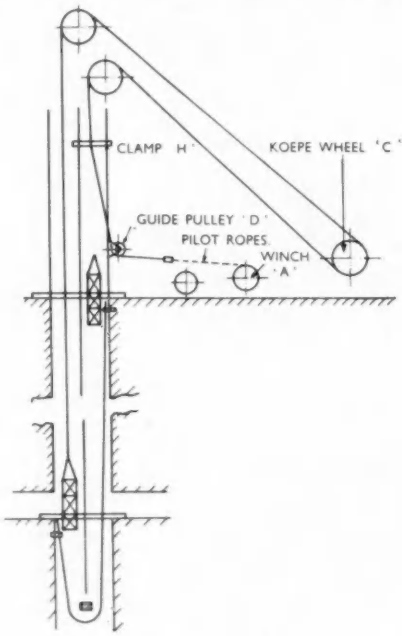

Fig. 39a.

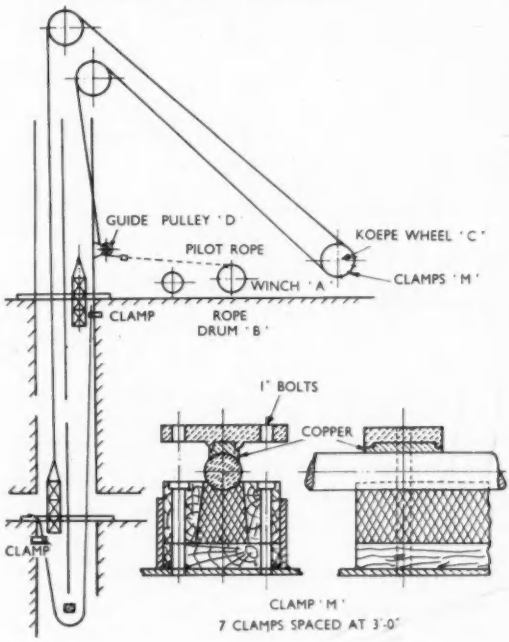

Fig. 39b.

Installation of ropes.

When the new rope is in position it is in turn clamped at *P* and *R*. The old rope is disconnected from the new rope which is then attached to the cages. Clamps *P* and *R* are taken away, together with the baulks supporting the cages.

Winding Rope.

The cages are supported on baulks (fig. 41) and the old rope held by clamps *G* and *H*, after which it is disconnected from the cages.

The new rope is connected to a pilot rope and wound from the rope manufacturers' drum *B* on to auxiliary winch *A*. The other end is then threaded under guide pulley *D* and attached to the old rope at *L*.

A pilot rope is connected to the other end of the old rope at *M* and clamps *G* and *H* released.

The winder and winch *A* are turned simultaneously, the new rope being unwound from this winch, while by turning drum *K* at pit bottom by hand, the old rope is wound on to it. The rope speed during this operation should be between 1·5 and 3·5 ft./sec.

Sometimes the old rope is drawn into the pit instead of winding it on to drum *K*.

Clamps *G* and *H* are re-connected, and the ends of the new rope now at *L* and *M* are detached from the pilot and old ropes respectively and connected to the cages. Rope clamps *G* and *H* are released, and the supporting baulks removed.

The same remarks regarding the position of the cages and length of rope apply equally here as in the case when the original ropes are installed.

The old rope now on drum *K* is raised to the surface. Should it be impossible to accommodate this drum in the cage, the rope is wound on to two smaller drums, one drum being placed on each of two decks of the cage. This procedure does away with the necessity of cutting the rope.

It is an advantage, when coiling the rope on to auxiliary winch *A*, to place sheet steel plates about 1/32 in. thick between the layers of rope, and thus prevent rope squeezing between the coils of the preceding layer, which would tend to damage the rope.

An alternative method of changing ropes which does away with the necessity of taking drum *N* (fig. 40) to pit bottom is as follows :

Winding Rope : Alternative Method.

Winch *A* (fig. 42) is placed as close as possible to the centre line of the shaft, and at a suitable level between banking level and the safety keps. The right-hand cage is supported by baulks at

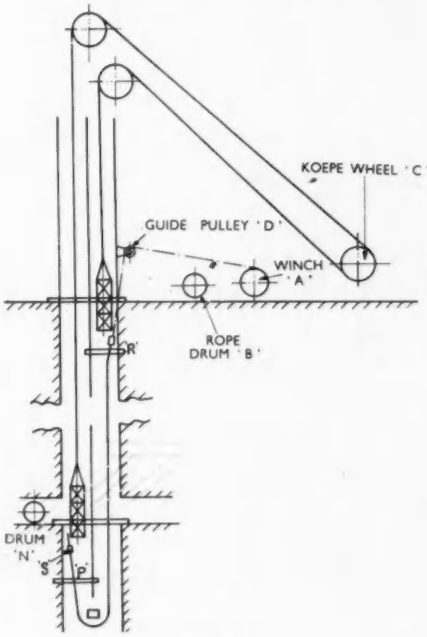

Fig. 40.

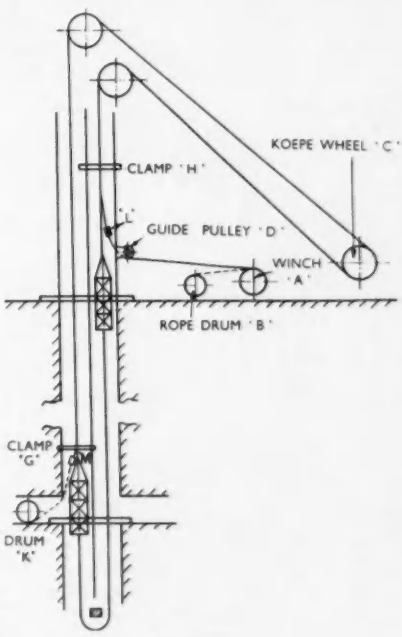

Fig. 41.

Installation of ropes.

bank level, and the winding rope clamped at *H* and detached from the cage. The end of the winding rope is then secured to the winch *A*. The lower cage is also supported on baulks and the rope secured to a suitable rider and detached from the cage. Clamp *H* is removed and the rope is wound on to the drum of winch *A*.

On reaching the surface the rider is suitably supported, the rope is clamped between the rider and the head sheave, and removed from the rider. It is then clamped to the new rope which is on the manufacturers' drum *B*. The clamp is removed, and the new rope is drawn by the old rope round the head sheave *D*, Koepe wheel *C* and head sheave *E*.

The new rope is now clamped between the right-hand cage and the head sheave *E* and disconnected from the old rope, care being taken that there is sufficient length of new rope to reach and be attached to the winch *A*. The old rope is removed from winch *A*, and coiled on to a suitable reel. The new rope can now be attached to the drum of winch *A*. The clamp above the right-hand cage is now removed, and the new rope wound on to winch *A*. After being unwound from the drum *B* the new rope is attached to the rider which is lowered down the shaft, where the rope is attached to the left-hand cage, and the rider removed.

The rope is clamped above the right-hand cage and the remainder removed from the drum, cut to the correct length and, after being capped, attached to this cage.

Balance Rope : Alternative Method.

To change the balance rope (fig. 43), the right-hand cage is drawn into the safety keps, and the winding rope clamped just above the cage or to the Koepe wheel as shown in fig. 39b. The balance rope is then clamped at decking level, disconnected from the cage and attached to winch *A*.

The other end of the balance rope is detached from the left-hand cage, lowered into the sump and a rider attached. According to the Mines Regulations, there should be sufficient distance between the bottom landing and the sump to allow the left-hand cage to descend when the right-hand cage is on the safety keps.

The old balance rope is now wound on to winch *A*, and afterwards uncoiled on to an old drum for disposal.

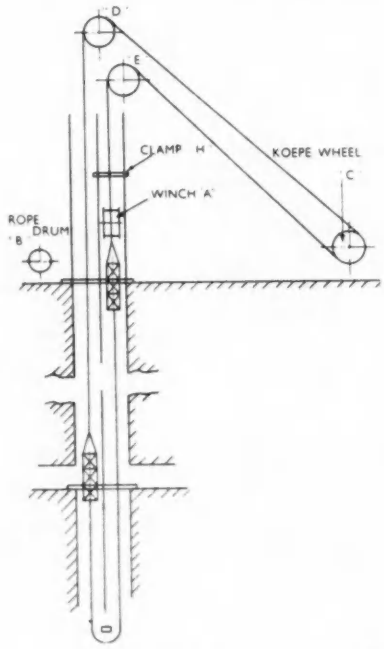

Fig. 42.

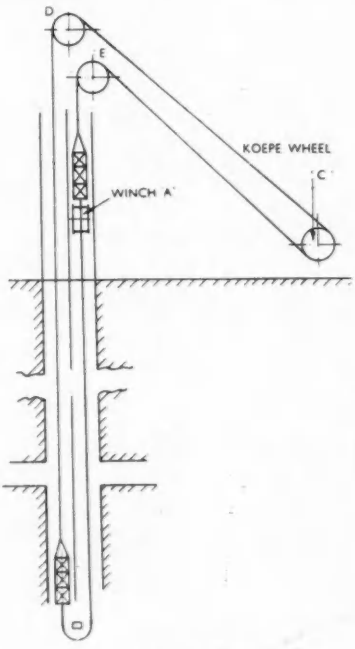

Fig. 43.

Installation of ropes.

The new balance rope is then wound on to winch *A*, and afterwards lowered down the shaft by a rider. At pit bottom a light pilot rope is attached, which is operated by a small winch at landing level for pulling the end of the balance rope round the guide beam. The rope is capped and attached to the left-hand cage.

At pit top the rope is clamped at decking level and removed from the winch *A*, capped and attached to the right-hand cage. The clamp is then removed.

Koepe Wheel with Rope Magazine. Installation of Original Ropes.

The other design of Koepe wheel, i.e. with a rope magazine, is shown in fig. 17, and one method used for changing ropes is as follows :

Balance Ropes.

A rope reel, *E* (fig. 44), with suitable brakes must be provided, and should be placed some 60 to 70 ft. away from the shaft. An auxiliary rope of sufficient length to reach from the guide pulley *D* to the Koepe pulley *A* is spliced or clamped to the free end of the tail or balance rope.

This pilot rope is then drawn to and clamped to the Koepe wheel.

The whole of the rope is slowly wound on to the Koepe wheel by means of the winder motor, while the rope reel *E* is being controlled by its brakes.

A pilot rope which is attached to the other end of the balance rope is threaded over jockey pulley *D*, and when the balance rope passes this pulley a suitable rider is attached. It is then lowered slowly down the shaft under control of the brakes of the winding engine, the rope speed being between 1·5 and 3·5 ft./sec.

On reaching the sump the rope is drawn by means of a chain tackle round the guide beam and up to the pit bottom.

The rope is then clamped at *F* and *G* (fig. 44), and the pilot rope detached from the rope and the Koepe wheel.

Winding Rope.

The winding rope reel *E*, fig. 45, is placed in position. A pilot rope is attached to the main rope, and is threaded round pulley *H*, over head sheave *C* to the Koepe wheel *A* to which it is clamped. The winder is now turned slowly and the winding rope is wound on to the wheel, until the rope is clear of pulley *H*. During the end period of this operation the pit head sheave *C* should be secured with a beam to prevent its

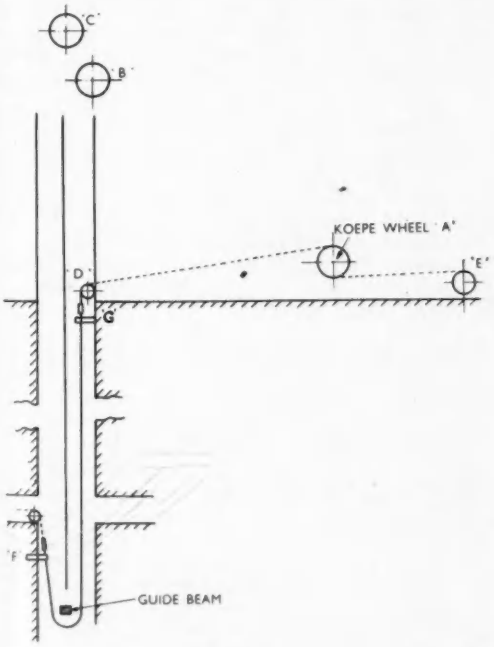

Fig. 44.

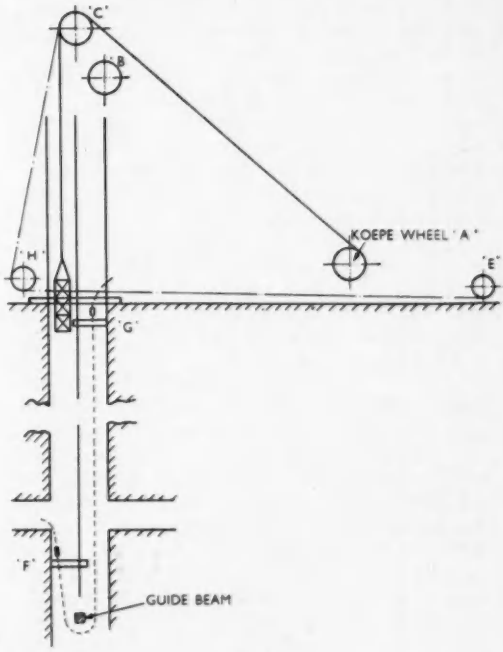

Fig. 45.

Installation of ropes.

turning so that it has a braking effect on the rope, the free end of which is kept taut by a pilot rope.

The left-hand cage is placed in position, and one end of the rope attached (fig. 45).

The cage is now slowly lowered down the shaft by the winding engine at a speed between 1·5 and 3·5 ft./sec. At pit bottom the cage is supported on baulks, and the tail rope attached (fig. 46). The winding rope is secured to the head frame above ground level by means of clamp *K*.

The remaining rope on the Koepe wheel *A* is now unwound by turning the winder very slowly, care being taken to ensure that the excess rope developed between pulley *A* and head sheave *C* is kept taut and controlled by a pilot rope.

The rope is now passed over the Koepe pulley and the free end is drawn by means of an auxiliary rope over the head sheave *B* and down to ground level. The cage is placed in position when the tail and winding ropes are attached (fig. 47).

The cages must be supported at exactly the correct distance apart when the final attachments are made, and the winding rope attachment gear must be shortened to compensate for the amount of rope stretch due to the depth of the shaft and the weight of load.

The depth indicator is then adjusted, the cages fully loaded and raised and lowered in the shaft to stretch the rope to its proper length.

Rope Changing.

The cages are supported on baulks, and the balance rope clamped at *G* and *F*, while the winding rope is clamped at *K* (fig. 46). The winding rope is then drawn over head sheave *B* and clamped to the Koepe wheel.

The top cage is removed and the winding rope slowly wound on to the Koepe pulley, clamp *K* being removed at the appropriate time. When the other cage reaches pit top it is suitably supported, and detached from the rope (fig. 45).

A pilot rope is clamped to the winding rope and the whole wound on to the Koepe wheel, after which it is unwound and removed.

A pilot rope is now attached to the balance rope, and after releasing clamps *G* and *F* is wound on to the Koepe wheel, from which it is ultimately removed. The new ropes are then installed as described above.

In the Ruhr District, Koepe winders without a rope magazine were the more favoured, the main reason being that the ropes could be changed in a much shorter time than with pulleys having a rope magazine.

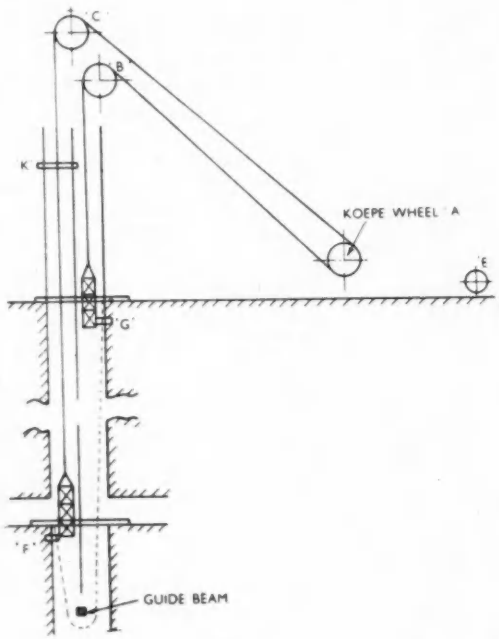

Fig. 46.

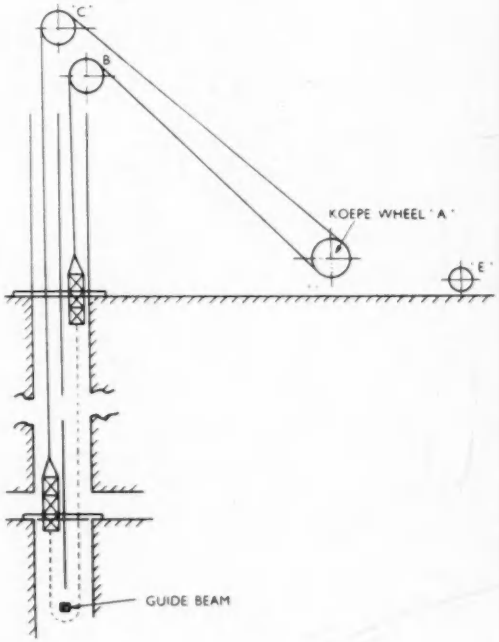

Fig. 47.

Installation of ropes.

X-Rays in the Development of Inorganic Phosphors

By H. P. ROOKSBY, B.Sc., F.Inst.P. and A. H. McKEAG, M.Sc., A.R.I.C.
G.E.C. Research Laboratories.

The paper was presented at a meeting of the Electrochemical Society held at Philadelphia, U.S.A., on May 5th, 1949, as a contribution to a Symposium on Luminescence. It gives a survey of the manner in which X-ray analysis has been used to evaluate different characteristics of inorganic phosphors.

It is becoming increasingly obvious that an extensive knowledge of the crystal chemistry of luminescent materials is required for practical development and improvement, and the contributions made by X-ray analysis in this subject are discussed.

INTRODUCTION.

OF recent years there has been much activity in the field of study of luminescent substances. Besides the desire on the part of chemists and physicists to arrive at a fundamental understanding of the phenomenon of luminescence itself, the important applications of phosphors in discharge lamps and cathode ray tubes have stimulated many technological investigations.

Both the development of a satisfactory physical explanation and the necessity for preparation of new phosphor materials with a high luminescent efficiency require that a number of contributory factors should be investigated. One of the most important aspects of phosphors to be studied is their crystal chemistry, and much valuable information on this question has been acquired through examination by X-ray methods. In this paper it is proposed to describe briefly some of the functions of X-ray analysis in this work, and to discuss the implications of some of the results obtained.

X-RAYS AND THE IDENTITY OF A PHOSPHOR PREPARATION.

The use of X-rays for the identification and specification of chemical preparations is so well known to-day, that there is little need to do much more than remark on its practical value. We shall be primarily concerned with the X-ray examination of powders, and diffraction patterns or crystal fingerprints of substances in powder form are of such general utility in identification work that a published reference card index is now available to X-ray workers.[1]

[1] Card File of X-ray Diffraction data published jointly by A.S.T.M. and National Research Council, 1942. See also *Jour. Sci. Inst.* 1945, *22*, 160, and A. J. C. WILSON.[1]

Two aspects of X-ray identification may be worth enlarging upon. In the first place in any new reacting system it should be practicable, by X-ray study, to determine how many compounds are formed and to ascertain the composition of each. Two examples may be given in illustration.

In an early investigation of cadmium phosphates in our laboratories the examination of the possibilities of these phosphates as luminescent powders was supplemented by X-ray studies. It was discovered that the particular preparation that had more favourable luminescent characteristics than others was one in which the impurity activator was added as chloride. The X-ray evidence confirmed the chemical evidence that chlorine was an essential ingredient and revealed that the promising phosphor was cadmium chlorophosphate, with molecular formula $3Cd_3(PO_4)_2.CdCl_2$. The crystal structure is isomorphous with that of apatite and it was through this analogy that the cadmium compound was recognised. Naturally when the composition is established it is possible to devise rational methods of preparation.[2]

The second example concerns the exploration of possible compounds formed between zinc oxide and boric oxide. In this instance a number of different compositions was studied, the impurity activator, manganese, serving to reveal which of the various phases were likely to be useful phosphors. Changing the composition over the range from a molecular ratio of ZnO to B_2O_3 of 3 : 1 to a molecular ratio 1 : 2 only gave three phases, specified by distinctive X-ray photographs. Only two of these, of molecular formulae $3ZnO.B_2O_3$ and $ZnO.B_2O_3$ respec-

tively, and whose X-ray patterns are illustrated in fig. 1 appear to have useful characteristics as phosphors. It is further noteworthy that the structural dissimilarity leads to entirely different luminescent colours; $3ZnO.B_2O_3$—*Mn* exhibits an orange-red fluorescence under short wave u.v. while $ZnO.B_2O_3$—*Mn* exhibits green fluorescence.

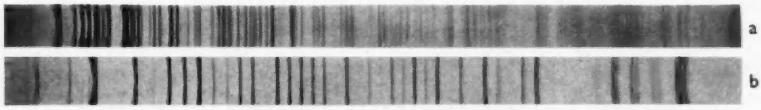

Fig. 1.—X-ray powder photographs of zinc borate phosphors (manganese activated). (a) $3ZnO.B_2O_3$. (b) $ZnO.B_2O_3$.

The second aspect of identification by X-rays may be appropriately mentioned at this point. One is enabled to distinguish quite unequivocably between polymorphic forms of a substance, if such exist. The distinction is as significant in luminescence as that between different compounds, as the luminescent properties will be in most instances profoundly influenced by the crystal structure.

For example, a considerable difference in the spectral distribution of fluorescence between zinc orthosilicates can be obtained depending upon the method of preparation. X-ray studies have revealed that the different fluorescent colours are associated with the formation of polymorphic varieties of zinc silicate.[3]

The more usual form of zinc silicate, corresponding with the mineral willemite, gives a strong green fluorescence when prepared in the presence of manganese as impurity activator. A distinctive zinc orthosilicate crystal structure, the β form, is obtained when preparations are made by rapid cooling from high temperatures, *circa* 1,450 degs. C., and in the presence of manganese the products give a yellow fluorescence under short wave u.v. The X-ray diagram is entirely different from that of the willemite form, and indicates the beta silicate to have a cristobalite-like crystal structure.[4] This beta silicate is also found, in a relatively poorly crystallised condition, in some low temperature preparations,[3] but as it is metastable with respect to willemite it is difficult to promote homogeneous formation, and X-ray investigations prove that rapid transformation to willemite occurs above about 900 degs. C. With manganese as activator a yellow fluorescent colour is given by the low temperature preparations, so long as no appreciable willemite formation is shown by X-ray examination.

Polymorphic forms of magnesium tungstate provide another interesting example. An X-ray investigation by Dunning and Megaw[5] has revealed the occurrence of at least two structural forms of the anhydrous tungstate. Only one of these forms, that stable in the temperature range 650 degs. C. to 1,050 degs. C. and having a characteristic monoclinic crystal structure, possesses luminescent properties, so that the significance of crystal form is very apparent in this instance. Our own X-ray data (fig. 2) indicate that, as in the case of zinc orthosilicate, low and high temperature preparations possess fundamentally similar crystal structures. The differences which are noticeable in the X-ray powder photographs are explicable in terms of differences in crystallinity, the magnesium tungstate formed in the temperature range 400 degs. C. to 650 degs. C. being in a much inferior state of crystallisation to that of the tungstate obtained at temperatures above 1,050 degs. C.

Fig. 2.—X-ray powder photographs comparing forms of magnesium tungstate obtained at different temperatures. Only the last form (800 degs. C., monoclinic structure) is fluorescent.

Apart from the use of X-rays to specify the chemical compound or distinguish a polymorphic

form, it is often desirable to furnish further simple crystallographic information concerning the crystal structure of the substance. This need not necessarily entail a complete solution of the structure, which cannot be accomplished very conveniently by X-ray powder methods except in simple cases, but with many crystals it should be possible to determine the lattice parameters and in some instances state the possible space group. For example, the relative simplicity of the X-ray pattern of the zinc metaborate phosphor (fig. 1b) shows the crystal structure to fall in a high symmetry space group, and an approximate solution of the structure could provide useful guidance to the arrangement of constituent matrix and activator atoms.

Certain other details of the X-ray powder photograph provide guidance on such matters as crystallinity and crystal perfection, matters which have certain significance in relation to luminescence, as will be indicated below.

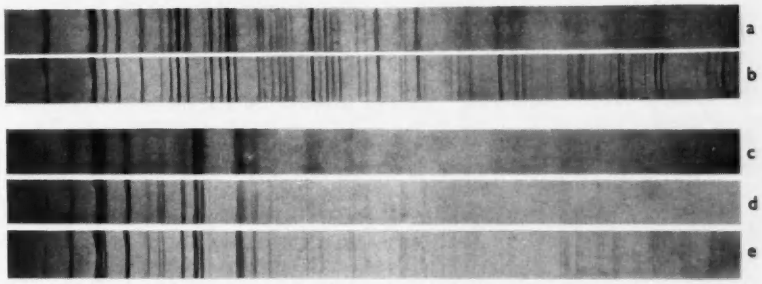

Fig. 3.—X-ray powder photographs illustrating the relation between crystal size and firing temperature of calcium tungstate and cadmium tungstate powders. (a) $CaWO_4$ precipitated. (b) $CaWO_4$ fired at 900 degs. C. (c) $CdWO_4$ precipitated. (d) $CdWO_4$ fired at 400 degs. C. (e) $CdWO_4$ fired at 700 degs. C.

X-RAYS IN THE EXAMINATION OF CRYSTALLINE PERFECTION.

The form of the X-ray diagram as regards line width and line definition is directly influenced by such factors as crystal size and crystal perfection. By careful examination of X-ray line broadening estimates of the size of the crystallites constituting a phosphor powder may be made and such modifications of the structure as are brought about by grinding and plastic deformation may be studied, at least qualitatively.

It is well known that some compounds, such as calcium tungstate, though not requiring a foreign impurity to promote luminescence, do require heat treatment before they become phosphors of practical utility. As precipitated, and oven-dried at low temperatures (say, 110 degs. C.), calcium tungstate is relatively poorly fluorescent under short wave u.v. excitation. After heating at 900 degs. C. in air it acquires a strong blue-violet fluorescence. X-ray measurements prove that there is a definite correlation between the luminescent efficiency and the crystal size developed in the phosphor (fig. 3).

One of the best examples is cadmium tungstate and a series of X-ray powder photographs for preparations fired at successively increasing temperatures is shown in fig. 3. For a crystal size of *c.* 50Å represented by fig. 3c the tungstate is only feebly luminescent at room temperature, either under X-ray or short wave u.v. excitation. For a crystal size of *c.* 1μ, represented by fig. 3e, the maximum luminescent effect is observed, while an intermediate efficiency is given by the specimen corresponding with fig. 3d.

Similar observations have been made in the case of zinc tungstate, and one is led to the conclusion that a substantial degree of perfection of the crystals of these compounds is required before the full phosphor properties are developed.

Contrarily a procedure which impairs the crystalline perfection of a phosphor and introduces gross distortions or strains into the crystal lattice will cause a deterioration in the luminescent properties. It is possible in some instances to detect the onset of severe plastic deformation

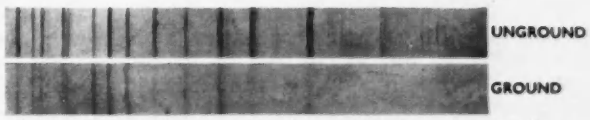

Fig. 4.—Parts of X-ray powder photographs illustrating the effects on line definition of grinding a zinc sulphide phosphor.

of the crystallites by observing the impairment of definition of X-ray reflections. With zinc sulphide, for example, severe grinding causes a rapid fall in the luminescent response, and as shown in fig. 4, X-ray line broadening occurs, revealing the presence of much lattice distortion, an effect additional to the fragmentation of the crystals that can be seen by visual inspection.

Similar results have been obtained with several phosphors, for example cadmium and zinc

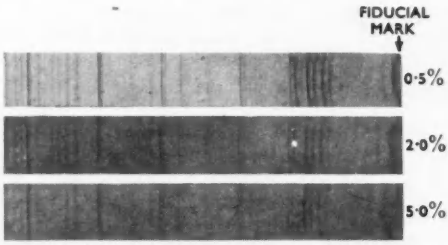

Fig. 5.—Parts of X-ray powder photographs of zinc orthosilicate phosphors containing successively increasing amounts of manganese.

tungstates, but with others, and particularly those in which it is difficult to induce deformation of the crystallites, for example willemite or other silicates, no very marked influence of grinding is observed. When profound flaws in the crystal lattice are introduced it is obvious that these must effect a serious disturbance of the active centres associated with the phenomenon of luminescence. Whether these active centres be impurity atoms, or particular groups, as in the tungstates, the critical arrangements of energy levels permitting the electronic transitions required by the luminescence effect will be upset. In some instances the situation can be restored by appropriate heat treatment, when both X-ray line definition is improved and some recovery of luminescent properties obtained. Because of the complex nature of the original chemical preparation and crystallisation, however, it is rather exceptional if the initial efficiency of luminescence is completely recovered.

THE ROLE OF THE IMPURITY ACTIVATOR IN LUMINESCENT COMPOUNDS.

The exact mechanism by which the activator becomes dissolved in the crystals of the matrix compound is of fundamental interest. The impurity may dissolve by the method of substitutional solid solution. In this event it occupies atomic sites and displaces atoms in the crystal lattice of the matrix material. Alternatively, if it is small enough, it need not directly replace metal atoms of the matrix, but can enter the space between them. In other words, it forms an interstitial solid solution.

Some direct evidence concerning the mechanism of solid solution of the activator has been obtained from X-ray analysis. It has been proved as a result of the examination of several manganese activated phosphors that the manganese does in fact substitute for atoms of the matrix lattice. In zinc orthosilicate, for example, the solid solution formation when the phosphor is prepared is revealed by a displacement of the X-ray reflections.[6] This is illustrated in fig. 5. The displacement observed corresponds with an expansion of the lattice dimensions as manganese is substituted for zinc. Such an expansion is to be expected from a consideration of the relative ionic sizes of the two elements. It is clearly necessary in preparing luminescent zinc orthosilicate to provide an excess of silica to combine completely with the added manganese, thus allowing isomorphous substitution of manganese for zinc in the orthosilicate structure. Coloration in the absence of this excess is attributable to manganese oxides for which no silica is available to provide the silicate compound necessary for solution in the zinc silicate structure.

It may be concluded that one of the important factors contributing to the wide usefulness of manganese as an impurity activator is the readiness with which it enters into solid solutions of the substitutional type with a variety of host compounds of divergent crystal structures. In the absence of an effective compounding of the manganese so that isomorphous replacement may take place, the development of luminescent properties becomes unlikely ; quite often discoloration of the preparation is noticeable.

Activators such as manganese which are predominantly metallic in character will presumably substitute mainly for the basic elements of the matrix. With other activators such as antimony and titanium which show amphoteric properties it is, however, more difficult to decide which position in the lattice the activator is likely to occupy, although ionic size considerations may give an indication in certain instances. This aspect is discussed later in the particular case of the calcium halophosphate phosphors activated with antimony and manganese.

The influence of the crystal structure of the host material on the spectral colour of fluorescence obtained with a given activator has already been referred to in earlier remarks on zinc borate compounds and the polymorphic forms of zinc silicate. Some further evidence has been obtained in the course of studies of uranium activated alkaline earth tungstates. Uranium, when it can be employed as an impurity activator, commonly

promotes a green luminescent colour. It does so, for example, in a group of tungstates recently described[7,8] which possess a pseudo-cubic type of crystal structure.

In tungstates of the $CdWO_4$, $ZnWO_4$ monoclinic class, however, uranium gives red luminescent effects. The $CdWO_4$—U phosphor is strongly red fluorescent at room temperature.[9] With $ZnWO_4$—U the red luminescence is weak at room temperature, but becomes strong and comparable with the effect from $CdWO_4$—U at liquid air temperature. Long wave u.v. (3,650Å) is the excitation medium.

The explanation appears to lie with the differences in crystal structure between the two classes of tungstate which are revealed by X-ray analysis. It is a reasonable assumption that the uranium atom substitutes for tungsten in the two types of structure. It is well established that in the monoclinic tungstates of the $CdWO_4$ class tungsten occurs in fourfold co-ordination with oxygen. We are thus likely to find uranium in the monoclinic structure surrounded tetrahedrally by four oxygens.

In the pseudo-cubic tungstates, of which the compound Ca_2MgWO_6 is an example, the X-ray evidence indicates that the tungsten atom is located within an octahedral group of oxygens. Uranium, substituting for tungsten, will thus be in sixfold co-ordination with oxygen, and it is with this UO_6 group that green fluorescence is associated.

This example directs attention again to the importance of knowledge about the manner in which the impurity activator substitutes in the matrix lattice.

EFFECT OF CHANGE IN COMPOSITION OF MATRIX ON COLOUR OF FLUORESCENCE

In discussing solid solution formation we have dealt so far only with small changes such as accompany the incorporation of an impurity activator into the matrix material. It is difficult to make a rigid distinction between the changes in structure accompanying activation by an impurity such as manganese and such changes in composition as alter profoundly the colour of the light emitted by the phosphor. It is noteworthy, for example, that, with zinc orthosilicate, increasing concentration of manganese orthosilicate moves the peak of the fluorescence slightly towards longer wavelengths. This is an instance of an impurity additive, whose primary function is activation, that at the same time modifies the spectral distribution of the fluorescence as its concentration is increased.

Much larger changes in composition through solid solution may result in more considerable modifications in the spectral distribution of the fluorescent light than result in the case of manganese activated zinc silicate. If instead of increasing the concentration of manganese we cause some of the zinc atoms to be replaced by beryllium atoms the spectral distribution is shifted from the green of willemite to yellowish-white, orange and red colours, depending upon the amount of manganese retained as activator. Valuable observations on the modifications of spectral colour of luminescence have been made by Leverenz and Seitz[10] and by Schulman.[11]

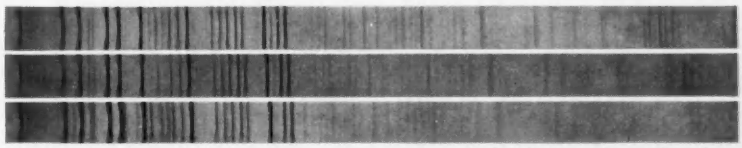

Fig. 6.—X-ray powder photographs comparing zinc orthosilicate and zinc beryllium orthosilicate phosphors. (a) Zinc orthosilicate. (b) Zinc beryllium silicate containing 13 molecular parts of Be_2SiO_4. (c) Zinc beryllium silicate containing 22 molecular parts of Be_2SiO_4.

X-ray analyses have shown the extent of the solid solution of beryllium orthosilicate in zinc orthosilicate under different conditions of treatment. The solution is accompanied by a lattice contraction and is thus in the opposite sense to that for solid solution of manganese silicate. Typical examples of X-ray powder photographs of zinc beryllium silicate phosphors are given in fig. 6. The X-ray measurements carried out by Fonda[12] and the authors have proved that the solubility of beryllium silicate varies with the temperature of preparation. At 1,350 degs. C. the limit of solid solubility is found to be in the order 25 molecular per cent, but at 1,050 degs. C. it is only some 15 molecular per cent. These limits are deduced from lattice parameter determinations. Furthermore, the solubility of the beryllium silicate is reduced in the presence of manganese.

Such observations explain why the luminescent colour changes are so much dependent upon the two factors, manganese content and firing temperature, during preparation. It is obvious

that a composition formed at a high temperature may be considerably modified by slow cooling or by a second heat treatment at a substantially lower temperature. Moreover, it has only to be remembered that the zinc beryllium silicate phosphors are mixed crystal phases containing three components, namely the orthosilicates of zinc, beryllium, and manganese, to realise that the situation is a complex one.

The zinc cadmium sulphide phosphors are very well known and provide an instance in which solid solution formation is possible in all proportions. It may be mentioned in passing that X-ray analysis is a quite accurate method of determining the molecular composition of any member of this solid solution series.[13]

One final instance of considerable importance in this class of materials has been discovered in recent years. A number of crystalline compounds of the structural type of apatite or calcium fluorophosphate has been developed by McKeag and Ranby.[14] All these compounds have been shown by X-ray examination to have the characteristic apatite crystal structure and a large number of variants have been prepared (figs. 7 and 8). The type compound has the formula $3Ca_3(PO_4)_2.CaF_2$ (or $Ca_5P_3O_{12}F$), but fluorine may be wholly or partially replaced by chlorine, and calcium may be replaced by strontium or barium.

Antimony has so far proved to be the most important of the primary activators, which include also tin, lead and bismuth. Antimony produces in the pure calcium fluorophosphate a pale-blue fluorescence reminiscent of magnesium tungstate. If the fluorine in this compound is replaced by chlorine a slight shift of the colour of fluorescence towards the green occurs.

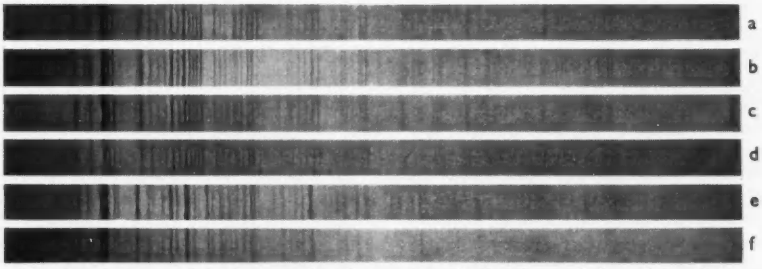

Fig. 7.—X-ray powder photographs of examples of phosphors of the calcium halophosphate class. (a) $3Ca_3(PO_4)_2.CaF_2$ with 2 per cent Mn, (b) $3Ca_3(PO_4)_2.CaF_2$ without activators. (c) $3Ca_3(PO_4)_2.CaF_2$ with 3 per cent Sb. (d) $3Ca_3(PO_4)_2.CaF_2$ with 3 per cent Sb, 2 per cent Mn. (e) $3Ca_3(PO_4)_2.CaCl_2$ without activators. (f) $3Ca_3(PO_4)_2.CaCl_2$ with 2 per cent Mn.

The introduction of manganese as a second activator produces a remarkable change in the luminescent effects obtainable from the phosphors. This element by itself gives no photoluminescence in the alkaline earth compounds ; in combination with antimony, however, it produces a wide range of colours depending on its concentration and the composition of the base material.

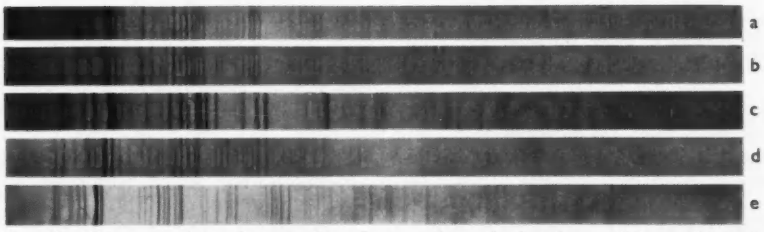

Fig. 8.—X-ray powder photographs of examples of phosphors with apatite-type crystal structure. (a) $3Ca_3(PO_4)_2.CaF_2$ pure. (b) $3Ca_3(PO_4)_2.CaO$. (c) $3Cd_3(PO_4)_2.CdF_2$, manganese activated. (d) $3Cd_3(PO_4)_2.CdCl_2$, manganese activated. (e) $3Ba_3(PO_4)_2.BaF_2$ with 3 per cent Sb, 2 per cent Mn.

It is interesting to compare the behaviour of manganese in these phosphors with its function in cadmium chlorophosphate.[2] In the latter compound which is also of apatite structure (see fig.

8) manganese, by itself, produces a strong yellow-orange fluorescence which is not dependent on the presence of other activators. Moreover, the spectral distribution of fluorescence shows little variation with concentration of manganese.

A progressive shift in the colour of the calcium fluorophosphates containing antimony is produced by the introduction of manganese in increasing amounts. This shift takes the colour from pale-blue to yellow as the manganese content is increased up to about 5 per cent by weight of the matrix. The colour of calcium chlorophosphate can be similarly modified by the introduction of manganese. In this case the colours range from greenish blue through pinkish white shades to orange pink with the higher amounts of manganese. Between these extremes of composition a wide range of shades can be produced depending on the fluorine to chlorine ratio in the matrix and on the manganese content.

The rôle of manganese is complex, because, not only does it behave as an impurity activator, but it also fulfils the function of modifying the composition and lattice dimensions of the matrix compound. Changes in lattice parameters can be demonstrated by X-ray powdered crystal examinations of members of this group of compounds. Structural isomorphism is conclusively established by the close relations between the line groupings, particularly in the low order regions. Some of the lattice parameter changes are of a much smaller magnitude than are found in the zinc beryllium silicate series or the zinc cadmium sulphides; this necessitates careful study of selected pairs of reflections to follow the small alterations occurring.

It is clear that replacement of fluorine by chlorine or calcium by strontium leads to an increase in the volume of the hexagonal structure cell. In the case of the halogen replacement the increase in volume occurs principally because of an extension of the a dimension of the hexagonal cell; the value of c_o shows a small contraction. With increasing manganese concentrations the structure cell dimensions decrease, and this is in accordance with ionic size considerations if manganese atoms replace calcium atoms in the structure. Figs. 7a, 7b and 7c compare X-ray photographs of synthetic calcium fluorophosphates prepared with and without manganese and antimony additions, and from these the magnitude of the X-ray line displacements occurring may be noted. The differences are consistent with random replacement of calcium by manganese in the manganese rich substance. X-ray photographs of other phosphors of the group are included in figs. 7 and 8, and demonstrate the order of the changes occurring on substitution of chlorine for fluorine and of other alkaline earth metals for calcium.

Alterations that result from the introduction of antimony into the pure calcium fluorophosphate compound are extremely small (figs. 7b and 7c), equivalent to changes in the lattice parameters of only a few parts in ten thousand. It is therefore difficult to decide on the probable positions occupied by the antimony atoms in the structure. As antimony possesses both marked basic and acidic properties, for example in the tetroxide $Sb^{III}Sb^{V}O_4$, replacement of either calcium or phosphorus appears possible. In the first instance a reduction in the volume of the structure cell should result, while in the second an increase would be expected. The possibility of substitution in both positions cannot be excluded.

A further series of phosphors has been prepared,[15] in which apatite-type structures are developed in the absence of halogen. In one method the compounds are fired in steam and sufficient excess calcium oxide is included to allow formation of either the hydroxy- or oxy-apatite compounds. The main activators for this new series are copper, antimony, tin and thallium.

It is remarkable how small the differences are between the X-ray data for the halogen free apatite-type compounds and fluor-apatite itself. X-ray patterns for fluor-apatite and one of the oxy-apatite preparations are compared in fig. 8; the structure cell dimensions are almost indistinguishable. As a result of the close similarity in the X-ray data, the distinction between hydroxy- and oxy-apatite formation is difficult, but the problem is being actively pursued. Slight modifications of the structure brought about by the introduction of other divalent oxides have formed the subject of a recent X-ray investigation by Brasseur.[16] He has succeeded in synthesising a considerable number of variants on the apatite structure.

REFERENCES.

1. Wilson, A. J. C., *Jour. Sci. Insts.*, *24*, 110 (1947).
2. McKeag, A. H., Randall, J. T., British Patent No. 495,706 (1937).
3. Rooksby, H. P., and McKeag, A. H., *Trans. Far. Soc.*, *37*, 308 (1941).
4. Weyl, W. A., *Jour. Appl. Phys.*, *17*, 628 (1945).
5. Dunning, N. J. and Megaw, H. D., *Trans. Far. Soc. 42*, 705 (1946).
6. Jenkins, H. G., McKeag, A. H. and Rooksby, H. P., *Nature*, *143*, 978 (1939).
7. McKeag, A. H., Ranby, P. W., British Patent No. 526,675 (1939).
8. Rooksby, H. P. and Steward, E. G., *Nature*, *157*, 458 (1946).
9. Levy, L. A., West, D. W., British Patent No. 528,828. 1939.
10. Leverenz, H. W. and Seitz, F., *Jour. Appl. Phys.*, *10*, 479 (1939).
11. Schulman, J. H., *Jour. Appl. Phys.*, *17*, 902 (1946).
12. Fonda, G. R., *Jour. Phys. Chem.*, *45*, 282 (1941).
13. Rooksby, H. P., *Jour. Sci. Insts.*, *18*, 89 (1941).
14. McKeag, A. H., Ranby, P. W., British Patent No. 578, 192. 1942.
15. McKeag, A. H., Ranby, P. W., British Patent Application No. 2142/48.
16. Brasseur, H., International Colloquium on Reactions in the Solid State. Paris, 1948.

Structure Testing Equipment at The Royal Aircraft Establishment Farnborough

By S. A. G. EMMS, B.Sc., Control Gear Department, Witton Engineering Works.

The testing of an aircraft structure is of fundamental importance as it is required to be only just strong enough. An overstrong structure does not imply greater safety.

The methods used in testing are necessarily complicated and the equipment intricate. The author describes the apparatus designed and built by the G.E.C. to the specification of The Royal Aircraft Establishment, Farnborough, by means of which the test loads are applied electrically and measured hydraulically. Both manual and automatic operation are available. In this way the work of testing is much simplified and the time required proportionately reduced.

INTRODUCTION.

ALTHOUGH the structural design of aircraft is complicated in detail, the essential requirements can be stated quite simply. The whole aim of the designer is to obtain a structure which is only just strong enough, as the cost of flying is such that no superfluous weight is permissible.

The worst conditions of flight can be calculated; the loads, thus computed, which these conditions impose on the structure of the aircraft are multiplied by an appropriate safety factor and the result used to determine the test loading figure.

The completed structure must fail at an applied load not appreciably in excess of that given by the safety factor. If, on a test to destruction, it is found that the aircraft, or part of it, is stronger than it need be, it is no matter for congratulation; for it means that the aircraft has excess material, redundant members and superfluous weight.

It must be understood that an overstrong structure does not imply greater safety. The surplus weight that has to be carried demands additional power and hence a heavier engine. This, in turn, requires a stronger and heavier structure and so the effect is cumulative. The result is an unduly heavy and cumbersome aircraft with no compensating advantage in the matter of safety. In other words, the correctly, and most efficiently, designed aircraft is one that is light, easy to manoeuvre and has the highest practicable safety factor. It is superior to the overstrong machine in respect of both performance and safety.

TESTING EQUIPMENTS AT THE R.A.E., FARNBOROUGH.

At the R.A.E., Farnborough there are two testing equipments, known as the " Cathedral " and " Abbey " respectively, for which the whole of the electrical equipment was designed and built at the Witton Works of The General Electric Co. Ltd. Both are similar except that the " Cathedral " is almost twice the size of the "Abbey".

Although some aircraft manufacturers have facilities for undertaking wing and fuselage testing on the scale of the " Abbey " equipment, the size of many aircraft at present in the prototype stage is such that something much larger is necessary. The " Cathedral " structure testing installation (fig. 1) meets this need. Some idea of its size can be obtained from the fact that the complete 120 ft. wing span of the Avro Lincoln aircraft was accommodated in it. The Bristol Brabazon tests, however, necessitated a half-scale model, which was comfortably installed in the 126 ft. long testing framework of the " Cathedral ". It may be added that the ecclesiastical names originate from the general appearance of an earlier rig which, owing to its numerous vertical members, became universally known as " The Temple ".

METHODS OF TESTING STRUCTURES.

Testing the strength of the structure of an aircraft is a complicated art and the equipment

used for the purpose is so intricate that its action is not always easy to understand. To give the reader a clear idea of the methods employed and the operation of the apparatus used it is proposed briefly to consider the fundamental principles involved.

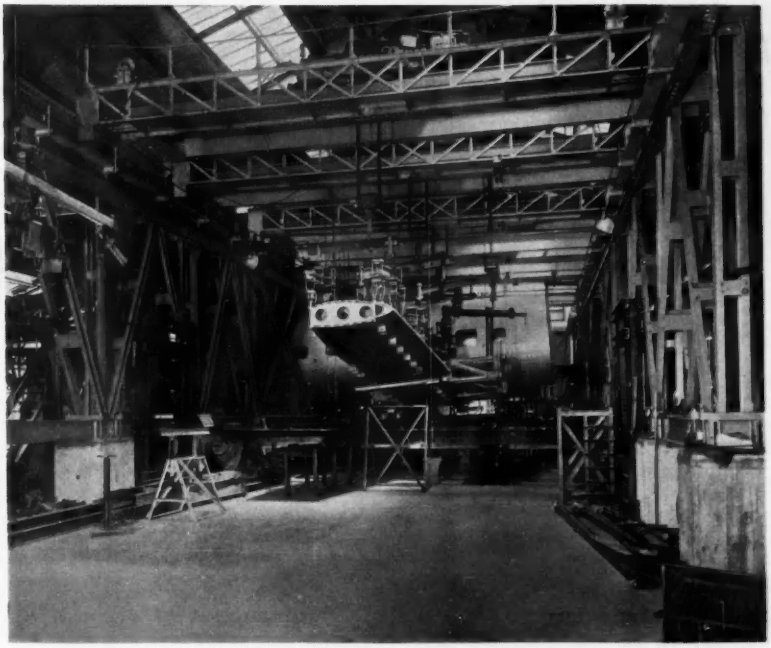

Fig. 1.—General view of the " Cathedral " installation with an aircraft set up for test.

At the outset it is necessary to understand what strength testing is. The main object is to reproduce the forces to which the structure is subjected in flight and apply them in the test laboratory. Loading is applied progressively in such a way that all the forces maintain as nearly as possible the same ratio to one another. In the course of a test the loading is carried beyond anything which should occur in flight, frequently to the point of fracture.

To reproduce exactly the conditions of flight the loads would have to be applied to the structure at an infinite number of points. As this is impossible, hundreds of forces are applied by the means of tension links attached to lugs specially built into the structure for the purpose. The forces are controlled by strainers attached to the rigid test frame. Fig. 2 shows diagrammatically the strainers and, below them, the system of linkages by means of which the forces are split up, or spread, so that they can be applied at a great number of different points on the structure. The strainers can be moved both laterally and longitudinally so that, for test purposes, they can be set to cover any desired area of the structure. Below the structure there are further strainers ; in some cases there may be attachment to dead anchorages. It will be noted that the system is shown rigged for vertical forces though it can be arranged, if necessary, to deal with forces in other directions.

Consideration must now be given to the type of strainer used to apply force to the structure. All forms of strainers can be divided into two classes : the reversible and the irreversible. The best example of the irreversible strainer is the screw jack ; the corresponding example of a reversible strainer is a hydraulic ram. It is important to note the fundamental difference between the two types. The reversible strainer gives direct control of force, displacement of the structure then follows in accordance with its elastic characteristics. Conversely, the irreversible strainer, namely the screw jack, directly controls displacement and force is controlled only indirectly, again according to the elastic behaviour of the structure.

It is beyond the scope of this article to give a

complete analysis of the characteristics of each type of strainer, but it is pertinent to note one or two ways in which they differ.

With a reversible strainer the rate of variation of force, and hence of displacement, must be restrained automatically. With the hydraulic ram this is done by introducing a high rate of velocity damping; nevertheless, when the structure fails, considerable further damage may be done before the force is removed. This may cause not only the loss of a valuable structure that might have been repaired and used again, but may conceal the nature and cause of initial failure. Also with this type of strainer static friction represents a direct error in the force applied.

By contrast the irreversible strainer is not significantly affected by friction, which merely makes the screw harder to turn; furthermore, at failure, the force is automatically removed and the structure preserved.

A careful appraisement of these and other characteristic differences in the behaviour of the two types of strainer shows that neither is entirely satisfactory for reasons that are fundamental. In some respects direct control of force is required; in others direct control of displacement. A compromise has therefore been adopted and a compound strainer is used which combines both the reversible and irreversible principles in such a way as to maintain so far as possible the advantages, and to eliminate the disadvantages, of both.

The compound strainer employed by the R.A.E. consists of a screwjack not mounted directly on the test frame but carried on a lever, the movement of which is restricted to a small amount by stops. When clear of the stops the lever is supported by a hydraulic ram as shown in fig. 3. Thus, while the system as a whole is irreversible, the strainer is reversible over the small range of travel permitted. A secondary ram is provided solely to balance the dead weight of the floating portion.

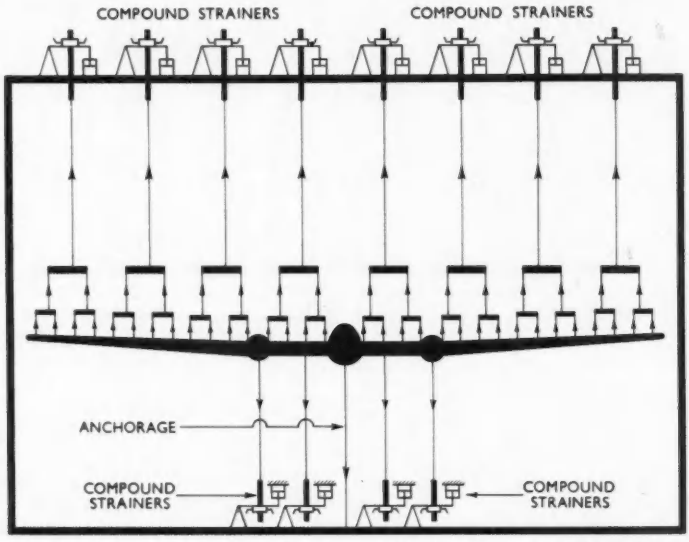

Fig. 2.—Diagram of aircraft structure under test showing strainers and system of linkages.

With this arrangement preliminary coarse adjustment of the screwjacks to make the levers float is not difficult. It does not in any way resemble the almost impossible task of obtaining a complete loading system by the use of screwjacks alone. Thereafter the entire system settles down automatically to give the desired forces as determined by the pressure applied to the rams.

To avoid the necessity of controlling the pressure in each ram separately, the leverages of all the rocking levers are so adjusted that at any stage of loading the pressures in the rams are required to be the same. The rams are then connected to a single pressure control; proportionality of loading is automatically ensured and only a single pressure needs to be controlled.

By means of the constant volume system used by the R.A.E. the rams are all interconnected, fluid which passes out of one ram must enter

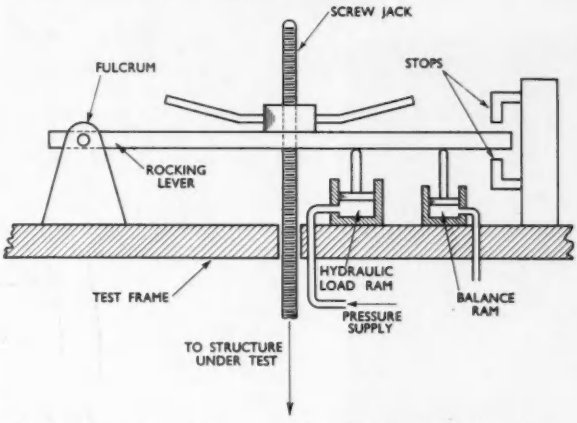

Fig. 3.—Diagrammatic representation of the compound strainer.

the others, and the volume of fluid is adjusted so that, roughly, it corresponds to all the rocking levers being in their mid-positions. Arrangement is made to compensate for leakage. In course of the subsequent adjustment of the screw jacks the operators are thus seeking an attainable condition.

Hence with the constant volume system the actual controlled loads are given a measure of collective irreversibility just sufficient to fix the structure, but without any risk of undue concentration of corrective and stabilising loads locally.

In later sections of this article it will be shown how this mode of load testing is applied in practice and a description is given of the electrical apparatus used for this purpose.

PREPARATION FOR A TEST.

The problem of spreading what is virtually one load over what, ideally, should be an infinitely large number of points of attachment to the structure to be tested, has already been considered in the previous section. In practice this is a lengthy and laborious task, and it often takes as much as two months to set up a test. A typical test arrangement is seen in fig. 4 which shows the way in which the loads imposed by the strainers are distributed by the system of linkages to as many points as may be deemed necessary.

It will be remembered that all the rams of the separate straining units are coupled together into a closed hydraulic system, any variation in the load on one ram affecting all of them. This

Fig. 4.—A typical test set-up, showing strainers and links.

arrangement solves the problem of load measurement as it enables the loads on all the strainers to be read on one hydraulic dynamometer.

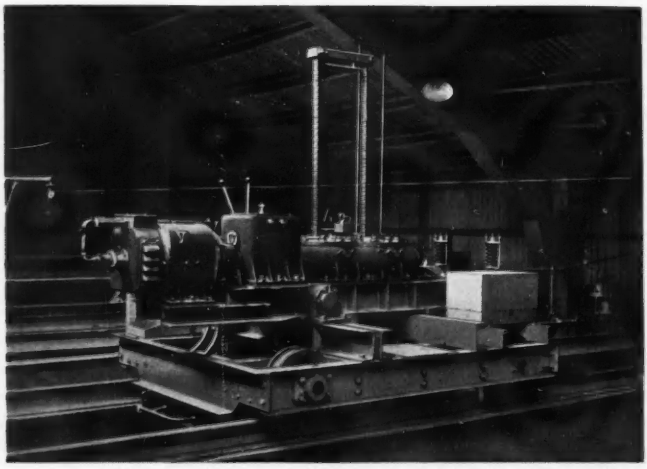

[Crown copyright reserved. Reproduced by permission of H.M. Stationery Office.

Fig. 5.—An overhead straining unit, showing the driving motor, variable speed gear box, reduction gear box and straining screws.

A further complication in rigging the test equipment arises from the relatively large differences in deflection which occur along the wing span from tip to root. To compensate for these differences each straining unit has three separate controls (1) the starting and stopping of individual motors as required; (2) the gear boxes, through which the straining units are operated, being set to ratios appropriate to the deflection anticipated; (3) the speeds of the motors which operate the strainers being varied during the application of the test load.

When a structure is finally rigged ready for test much other measuring equipment is used besides that required to determine the main loading. Strain gauges are attached to the skin of the aircraft, and as many as 600 may be employed on one test. As the test proceeds the behaviour of the structure, as measured by the strain gauges, is indicated on a cathode ray oscillograph which is switched through the range in high-speed sequence and recordings made by a ciné-camera.

APPLICATION OF LOAD.

The application of load in an actual test will now be considered. For the "Cathedral" installation, which is illustrated in fig. 1, there are eight overhead and four ground type straining units, each capable of exerting a maximum load of 18¾ tons. In the case of the overhead units the equipment is mounted on a carriage which is supported on a 30 ft. gantry spanning the width of the test frame (fig. 5). The arrangement is similar to that of an overhead crane and allows the straining unit to be placed anywhere within its prescribed operational area.

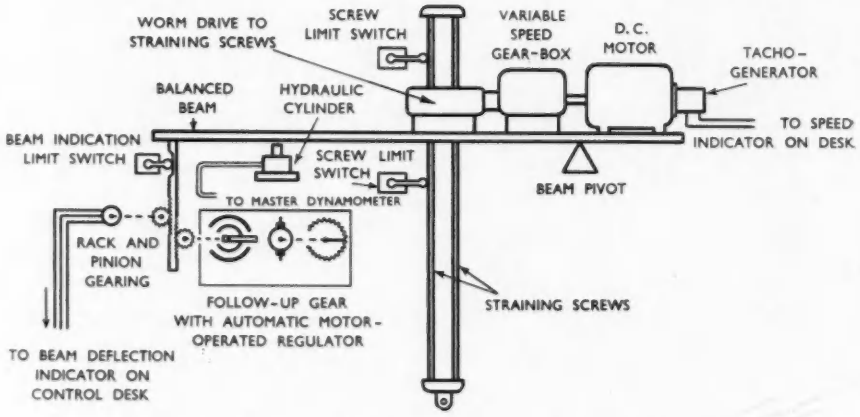

Fig. 6.—Arrangement of the electrical components of a straining unit.

The layout of the various components seen in fig. 5 is shown diagrammatically in fig. 6. Each straining unit consists of a motor for operating the straining screws, a hydraulic ram for balancing and measuring the load, and an automatic regulator for controlling the speed of the motor. The second ram, which balances the dead-weight of the testing equipment, derives its power from hydraulic accumulators. The load is thus applied electrically, the motor operating the straining screws through a variable speed gear box and spur and worm reduction gearing.

The motor is a variable speed 4 h.p. compound wound machine with a speed range from 820 to 1,700 r.p.m. which gives rates of travel of the screws from 1·07 ins. to 13·06 ins. a minute. A tacho-generator mounted on the motor shaft provides remote speed indication, and beam deflection is relayed by a transmitter to a remote indicator. A cut-out device affords protection against over-speeding of the motor and two sets of limit switches are fitted, one to prevent overrunning of the screws in either direction and the other to control the "beam up" and "beam down" indicator lamps.

Fig. 8.—Detail view of a control desk, showing arrangement of the equipment.

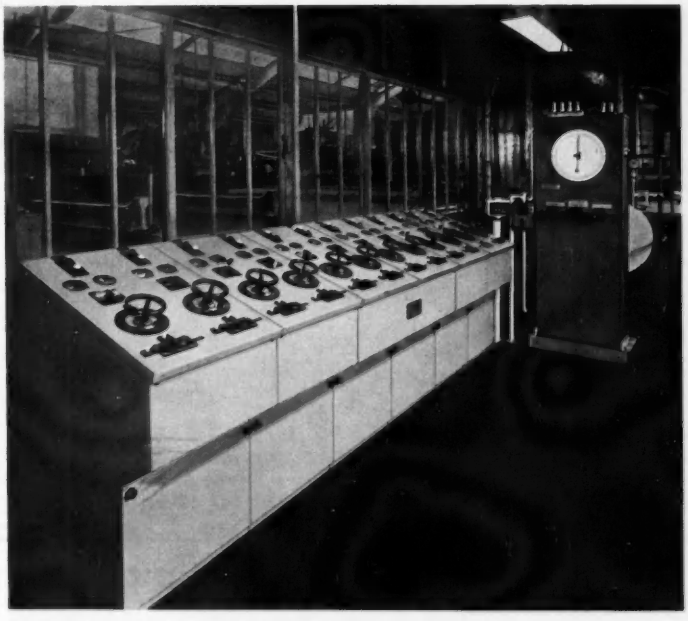

Fig. 7.—Control cabin, showing the main control desk and hydraulic dynamometer with master control push buttons alongside.

ELECTRICAL CONTROL GEAR.

The equipment is controlled from a cabin (fig. 7) in which is installed a control desk with twelve sets of equipment (one for each straining unit) and the hydraulic dynamometer, the contactor cubicles for the motors being situated immediately outside the control cabin.

The arrangement of the control equipment for each straining unit is shown in fig. 8. It includes "strain", "unload" and "stop" push buttons with indicator lamps; a field regulator; a selector switch for hand or automatic control; a beam deflection indicator; a motor speed indicator, and two indicator lamps to show whether the beam is against the upper or lower limit stops.

The equipment can be operated manually from each individual strain unit control panel or automatically from a central

point alongside the dynamometer, manual operation being the more frequently employed. Straining control can be continuous throughout the test range, but it has been found more convenient to apply the proof load in 10 per cent increments, taking readings at each stage. A schematic diagram of the connections for the control gear is seen in fig. 9.

MANUAL CONTROL.

For manual control, the automatic regulators on the straining unit are rendered inoperative, and the selector switches on the control desk are turned to " hand control ". The operators endeavour to vary the speed of the motors by means of the field regulators to compensate for the deflection of the aircraft structure, and the consequent hydraulic out-of-balance which is indicated by the individual beam positions. The general aim is to keep these beams in balance throughout the test.

AUTOMATIC CONTROL.

When this form of control is used, the automatic regulators on the straining units (fig. 10) are brought into service, and the selector switches on the control desk are turned to " auto-control ". This brings into operation the master " strain ", " unload " and " stop " push buttons, which are situated immediately beside the dynamometer.

Once the motors start to operate, the straining screws begin to apply force, causing a deflection in the structure. Small departures from the amount of deflection anticipated cause the load rams to move from their mean positions and the beams to tilt. As soon as any beam moves, a rack and pinion gear actuates a drum type switch

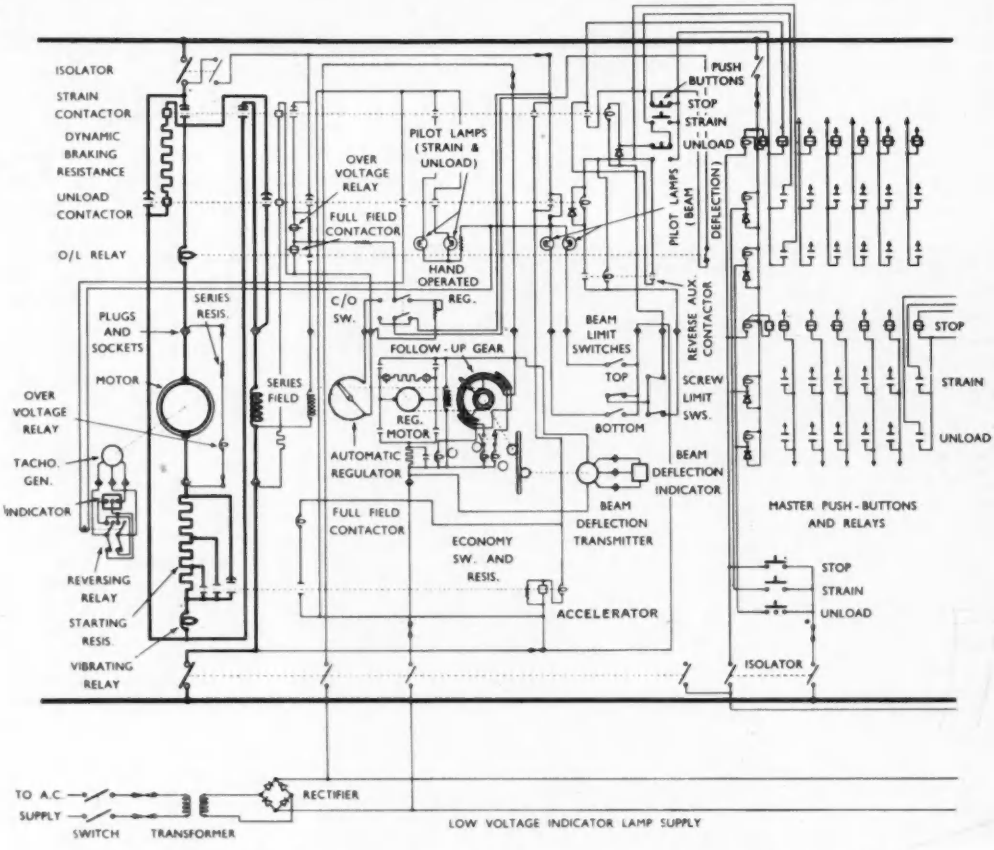

Fig. 9.—Schematic diagram of connections for the control gear of " Cathedral " and " Abbey " testing plants.

which operates a motor-driven field regulator and this increases or decreases the speed of the strain motor. When the strain motor reaches its correct speed it brings the beam back into balance thus switching off the automatic field regulator, and the strain motor continues to run at its new corrected speed.

TEST PROCEDURE.

A senior structural engineer acts as controller-in-charge, and is responsible for the method of installing the testing equipment and for the individual tests. From his elevated post he can supervise the whole operation and, if necessary, can stop the test immediately failure begins.

A floor supervisor is in charge of all recordings of structure movement and deflection. He has a measurement crew of specially trained observers, each man having a well-defined section to cover and subject to strict discipline, to ensure that the behaviour of every part of the structure is properly recorded.

At predetermined intervals the controller in charge announces by loudspeaker: "Readings at 20 per cent", or whatever it may be. The next ten or fifteen minutes are taken up by examination of scales, strain gauges and the appearance of the skin and rivets.

Simultaneously with the progressive loading of the main structure it is necessary to watch the behaviour of the skin. Wrinkles appear, their character and relative time of appearance are so important that unusually powerful lighting is arranged to show them in high relief and with such brilliance as to permit of repetitive photography at various stages throughout the test.

Tests are carried to destruction and can be spectacular. There is something like 100 foot-tons of energy stored up in the average fuselage and wing when under test; if the eventual failure takes place completely unexpectedly the test links can break up and shower down on the measurement crew below.

On the other hand, if obvious signs of failure are evident before proof loading is reached, and failure can be arrested before much damage is done, the manufacturers of the aircraft make suitable repairs and the test is continued later. This procedure may be repeated until the final failure occurs at a satisfactory loading figure slightly in excess of the proof load.

ACKNOWLEDGMENTS.

In conclusion it should be mentioned that Richard Sizer & Company, Ltd., of Hull, acted as main contractors for the mechanical equipment. The general specification for the complete installation was prepared by the Structures Department of the Royal Aircraft Establishment, and acknowledgment is due to the Chief Scientist, Ministry of Supply, for permission to publish the foregoing information. Acknowledgment is also made to P. B. Walker, M.A., Ph.D., and the Institution of Structural Engineers for material obtained from his paper "The Principles of Aircraft Strength Testing" published in the *Structural Engineer*, November, 1948.

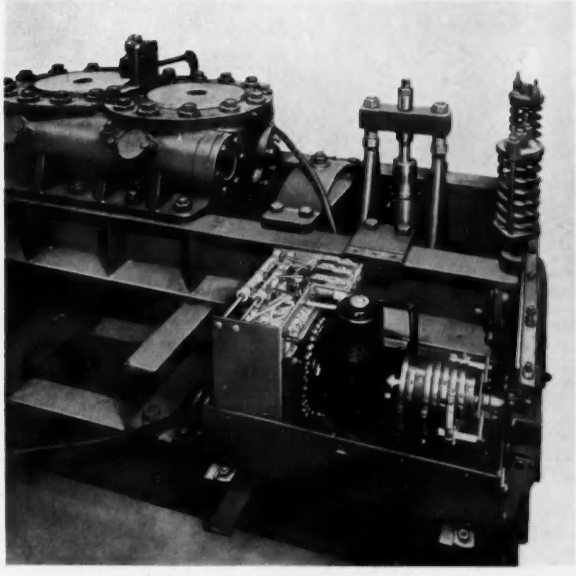

Fig. 10.—Automatic motor-driven regulator mounted on the straining unit.

TECHNICAL LITERATURE

A DIGEST OF RECENT BOOKS, ARTICLES AND PAPERS, BY MEMBERS OF THE G.E.C. AND ITS ASSOCIATED COMPANIES.

ATMOSPHERIC ABSORPTION OF MILLIMETRE WAVES (409).*

By H. R. L. Lamont (Research Laboratories).

Proc. Phys. Soc., Vol. 61, p. 562, 1948.

The attenuation of electromagnetic waves in the region of 5 mm. wavelength due to resonance in the oxygen molecule was measured over atmospheric paths up to 2 kms. long, using a fixed transmitter and a mobile superheterodyne receiver. For ten wavelengths between 6·34 and 4·48 mm. values were obtained which, after reduction to standard dry atmospheric conditions, range up to a maximum of 15·7 db/km. at the peak of the absorption curve. They agree substantially with the theory of Van Vleck, and give a value of line-breadth constant of about 0·02 cm.$^{-1}$ confirming estimates derived from other methods.

DESIGN OF CONTACT LIGHTS FOR AERODROME RUNWAYS (411).*

By H. J. Turner (Research Laboratories).

Trans. I.E.S., Vol. 14, No. 1, 1949.

An account is given of methods of calculating the light distribution required from aerodrome runway contact lights with particular reference to foggy weather. The limitations on intensity and light distribution imposed by mechanical and electrical conditions and the relative merits of flush-mounted and elevated lights are discussed. Consideration is given to the light distribution in directions other than those from which the lights are seen during approach and landing.

THE DESIGN OF SPECIAL CIRCUIT FOR HIGH INTENSITY DISCHARGE LAMPS (413).*

By V. J. Francis and A. H. Willoughby (Research Laboratories).

Proc. I.E.E., Vol. 96, Part II, No. 50, April, 1949.

High intensity high pressure mercury vapour (h.p.m.v.) lamps are now being used in cinema studios and for other important applications. During the development of lamps and circuits suitable for these purposes, it was necessary to solve circuit difficulties of a rather special nature, and it is the purpose of the paper to discuss these problems. Fairly complete descriptions are also given of some of the circuits which experience has shown to be suitable for commercial use. Although most of the lamps towards which the discussion is directed are of the high pressure mercury vapour type, the principles are often of much wider interest and application.

THEORY OF THE HIGH PRESSURE MERCURY VAPOUR AND CADMIUM VAPOUR DISCHARGES (415).*

By V. J. Francis (Research Laboratories).

Phil. Mag., Ser. 7, Vol. XL, p. 435, April, 1949.

The characteristics of the high pressure discharge in cadmium vapour are calculated from fundamental principles. The constants and parameters required in this calculation are obtained by comparing the results with similar curves for mercury, for which these parameters are known with greater accuracy and for which many more data are also available. The cadmium characteristics are compared with experimentally determined data and satisfactory agreement is obtained.

FREE BARIUM AND THE OXIDE CATHODE (419).

By R. O. Jenkins and R. H. C. Newton (Research Staff of the M.O. Valve Co. Ltd. at the G.E.C. Research Laboratories).

Jour. Sci. Insts., Vol. 26, No. 5, May, 1949.

It is shown that the greater part of the free barium produced by a modern oxide-coated cathode is formed through chemical reduction by the impurities in the nickel core. The actual amount of free barium retained by the cathode may only be of the order of a tenth of that produced, the rest being evaporated on to other electrodes. There appears to be a lower limit to the rate of production at a given temperature, below which the emission cannot be maintained at a high level. The free barium concentration in a well-activated coating is of the order of 0·01 per cent or 3×10^{17} atoms/c.c.

HIGH INTENSITY METAL VAPOUR DISCHARGE LAMPS (421).*

By E. H. Nelson (Research Laboratories).

Photographic Jour., Section B., Vol. 88B, 1949.

After a short historical introduction, recent developments of continuous burning high intensity metal vapour discharge lamps are discussed. The paper describes types of lamps now coming into use and also experimental lamps at present being investigated, thus indicating the probable trend of lamp design in the future.

RESEARCH IN THE NON-FERROUS FIELD CARRIED OUT AT THE RESEARCH LABORATORIES OF THE GENERAL ELECTRIC COMPANY LIMITED (425).*

By I. Jenkins (Research Laboratories).

Metal Treatment, Spring, 1949.

Because of the extensive use of non-ferrous metals in electrical equipment and appliances, the metallurgical problems which arise are many and varied and, in many cases, outside those which normally confront the metallurgical industries. Work of this nature carried out at the G.E.C. Research Laboratories is described.

AERODROME LIGHTING.

By W. A. Villiers (G.E.C. Exterior Lighting Department).

The Aeroplane, August 12th and 19th, 1949.

This article discusses the aerodrome lighting requirements dictated by the developments of flying technique, aircraft and aerodromes which have taken place during and since the recent war. British and American systems of approach and runway-lighting are described and the general discussion is followed by an illustrated description of the various lighting units at present in production.
This article forms a useful guide for all those interested in providing visual night landing facilities in accordance with the current international recommendations.

***A limited number of reprints is available of those papers marked with an asterisk. Copies may be obtained on application to the Editor, G.E.C. Journal, Magnet House, Kingsway, W.C.2.**